RESEARCH AND DEVELOPMENT TECHNICAL REPORT
ECOM-5812

APPLICATION OF THE AN/GVS-5 LASER RANGEFINDER TO CLOUD BASE HEIGHT MEASUREMENTS

By
Robert S. Bonner
R. Newton

Atmospheric Sciences Laboratory
US Army Electronics Command
White Sands Missile Range, New Mexico 88002

February 1977

Approved for public release; distribution unlimited.

ECOM
UNITED STATES ARMY ELECTRONICS COMMAND - FORT MONMOUTH, NEW JERSEY 07703

NOTICES

Disclaimers

Disposition

SECURITY CLASSIFICATION OF THIS PAGE (When Data Entered)

REPORT DOCUMENTATION PAGE

READ INSTRUCTIONS BEFORE COMPLETING FORM

1. REPORT NUMBER: ECOM-5812	2. GOVT ACCESSION NO.
	3. RECIPIENT'S CATALOG NUMBER
4. TITLE (and Subtitle): APPLICATION OF THE AN/GVS-5 LASER RANGEFINDER TO CLOUD BASE HEIGHT MEASUREMENTS	5. TYPE OF REPORT & PERIOD COVERED
	6. PERFORMING ORG. REPORT NUMBER
7. AUTHOR(s): Robert S. Bonner, R. Newton	8. CONTRACT OR GRANT NUMBER(s)
9. PERFORMING ORGANIZATION NAME AND ADDRESS: Atmospheric Sciences Laboratory, White Sands Missile Range, New Mexico 88002	10. PROGRAM ELEMENT, PROJECT, TASK AREA & WORK UNIT NUMBERS: DA Task 1L162111AH71A380
11. CONTROLLING OFFICE NAME AND ADDRESS: US Army Electronics Command, Fort Monmouth, New Jersey 07703	12. REPORT DATE: February 1977
	13. NUMBER OF PAGES: 45
14. MONITORING AGENCY NAME & ADDRESS (if different from Controlling Office)	15. SECURITY CLASS. (of this report): UNCLASSIFIED
	15a. DECLASSIFICATION/DOWNGRADING SCHEDULE

16. DISTRIBUTION STATEMENT (of this Report)

Approved for public release; distribution unlimited.

17. DISTRIBUTION STATEMENT (of the abstract entered in Block 20, if different from Report)

18. SUPPLEMENTARY NOTES

19. KEY WORDS (Continue on reverse side if necessary and identify by block number)

Ceiling measurements
Portable laser rangefinder

20. ABSTRACT (Continue on reverse side if necessary and identify by block number)

Current portable instruments utilizing a bistatic technique for measuring cloud-base heights are subject to large errors when the ceiling is greater than five times the instrument baseline.

A hand-held, portable, low-cost, battery-operated laser range finder was evaluated for use as a cloud-base height instrument. The performance of the device was compared with the results obtained from several instruments designed

20. ABSTRACT (cont)

as ceilometers, an AN/GMQ-13A rotating beam ceilometer, an Impulsphysik ceiloskop, and an ASEA ceilometer. For ceilings between 80 and 400 meters, data from all instruments showed the same long-term trends and similar short-term variators. For ceilings above 400 meters, the ceiloskop showed large errors compared to the other ceilometers; while the readings obtained from AN/GMQ-13A, the ceilometer, and the AN/GVS-5 compared favorably.

PREFACE

The authors express their gratitude to Dr. Jack Smith, University of Texas at El Paso, for his assistance in editing this report and to Major Thomas O. Carmichael, CDR, and personnel of Detachment I, 24th Weather Squadron, Randolph AFB, TX.

CONTENTS

INTRODUCTION

Cloud-base height measurements are desirable not only at the larger permanent airfield installations, but also in tactical situations at temporary or small remote locations requiring air support.

While the current instrumentation is suited for cloud-base height measurement at permanent installations, a portable instrument suited for use at temporary or remote locations has not been fully developed. The height measurement can be made by using a bistatic technique. This requires a baseline of several hundred feet and rather precise mechanical alignment of the system [1, 2]. More recent instrumentation developments provide a single-ended system [3, 4]. Although they overcome the baseline and mechanical alignment problems, these units are large and cannot be battery operated for any extended period of time. The results of testing single-ended relatively large laser ceilometers with a standard rotating beam ceilometer were reported by Moroz, Lawrance, and Travers [5]. To overcome the size and power problem, the authors suggest that it would be feasible to modify the small, portable, battery-operated AN/GVS-5 laser range finder to provide cloud-base height measurements.

The objective of this study was to establish the performance characteristics of the AN/GVS-5 when used as an instrument for measuring cloud-base height. This objective was accomplished by comparing results obtained with the results from several conventional cloud-base height instruments, a rotating beam ceilometer (AN/GMQ-13A), an Impulsphysik ceiloskop, and an ASEA ceilometer. The rotating beam ceilometer and ceiloskop are bistatic instruments that measure cloud heights by triangulation. Both use noncoherent light sources. The AN/GVS-5 and the ASEA are monostatic instruments that measure cloud heights by time lapse from transmitted to detected signal.

The basic specifications for the AN/GVS-5, as well as the other three instruments mentioned, are listed in Appendix A.

INSTRUMENT DESCRIPTION

AN/GMQ-13A Rotating Beam Ceilometer

The rotating beam ceilometer (RBC) is a widely used instrument at fixed installations. It consists of transmitter and receiver units separated by a determined baseline (Fig. 1). The projecting optics are rotated, while the receiver field of view is vertical and coplanar with the rotating projector beam. A cloud in the common volume produces a backscattered signal which is detected by the receiver. Cloud height is then determined by triangulation.

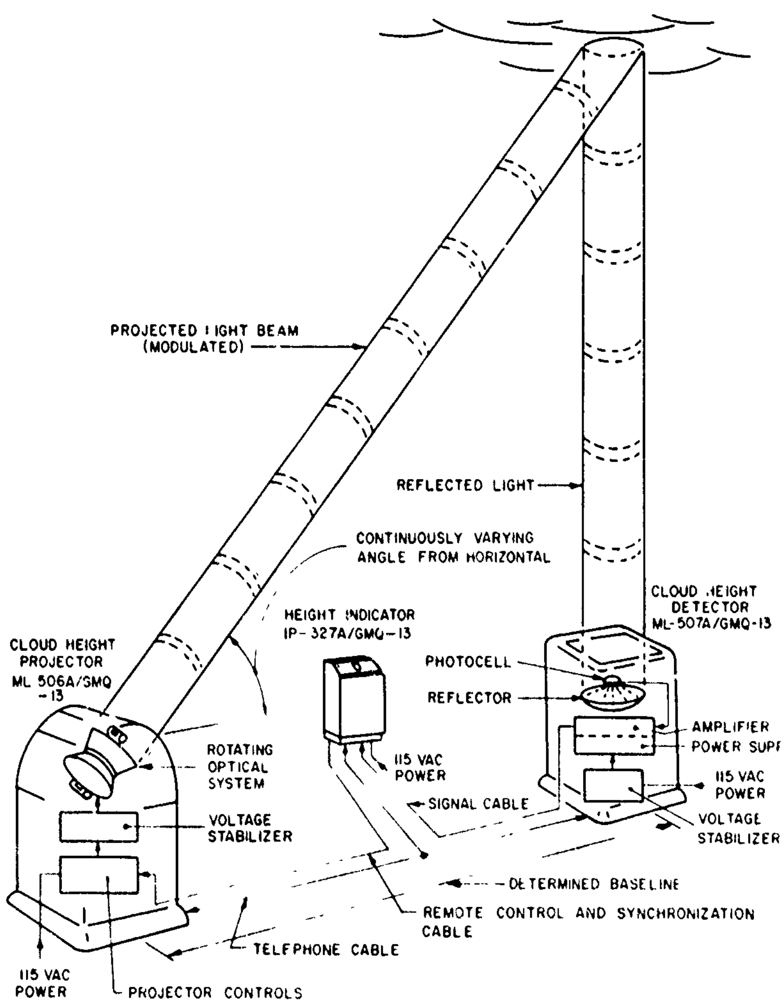

Figure 1. System block diagram.

The RBC is limited to use at installations where the necessary baseline is available and the mechanical alignment can be established and maintained. In addition, the transmitter and receiver units are quite bulky, approximately 700 pounds each.

Impulsphysik Ceiloskop

The ceiloskop uses a bistatic geometry for the measurement of cloud-base height. Its baseline is 25 meters. The projector is fixed in a vertically aimed position and projects a modulated (3 pulses per second) beam toward the cloud base (Fig. 2). The detector is leveled on its tripod while in the 0-degree elevation angle position and while it is aimed toward the projector. The elevation angle is indicated in the small window in the carriage of the detector. The detector is then rotated toward the vertical in a plane containing the baseline until the modulated beam on the cloud base is detected. A small neon bulb and an audible pulse indicator are activated when the beam is detected. The angle of inclination is read and recorded by the operator at this first indication. The detector aim is then moved to the opposite side of the beam spot and another angle of inclination is noted. The average of the two angles of inclination noted on opposite sides of the beam spot is taken as the angle of inclination to be used in the cloud-base height calculation. The baseline and angle are then used in the calculation of the cloud-base height.

ASEA Type QL-1210 Ceilometer

The ceilometer is a Swedish made lidar using a colocated transmitter and receiver (Fig. 3). Its principle of measurement is the same as the AN/GVS-5; however, there are some basic differences. Its transmitter is a 1.3 microjoule per pulse - 2000 pulse per second GaAs diode laser (wavelength 906 nanometers). This low energy makes the device less hazardous for the eyes of personnel. Each sampling sequence is automatically trigerred at 75-second intervals. The actual measurement cycle lasts only the first 30 seconds of each interval. Its measurement range is 10 to 1000 meters. When the laser is triggered, a signal is simultaneously sent to a remotely located chart recorder. This signal starts the writing pen on the recorder moving toward the maximum indicated height on the chart paper (1000 meters). When a reflected signal from the cloud base is detected, a write signal causes the pen to mark the chart paper.

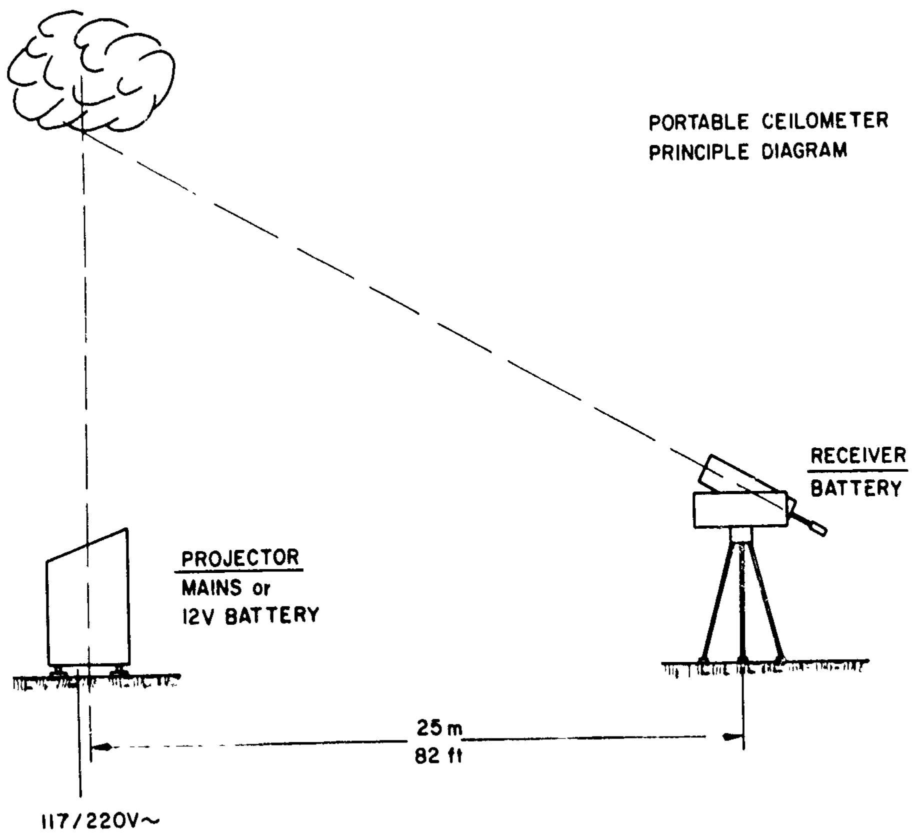

Figure 2. Diagram of ceiloskop operation.

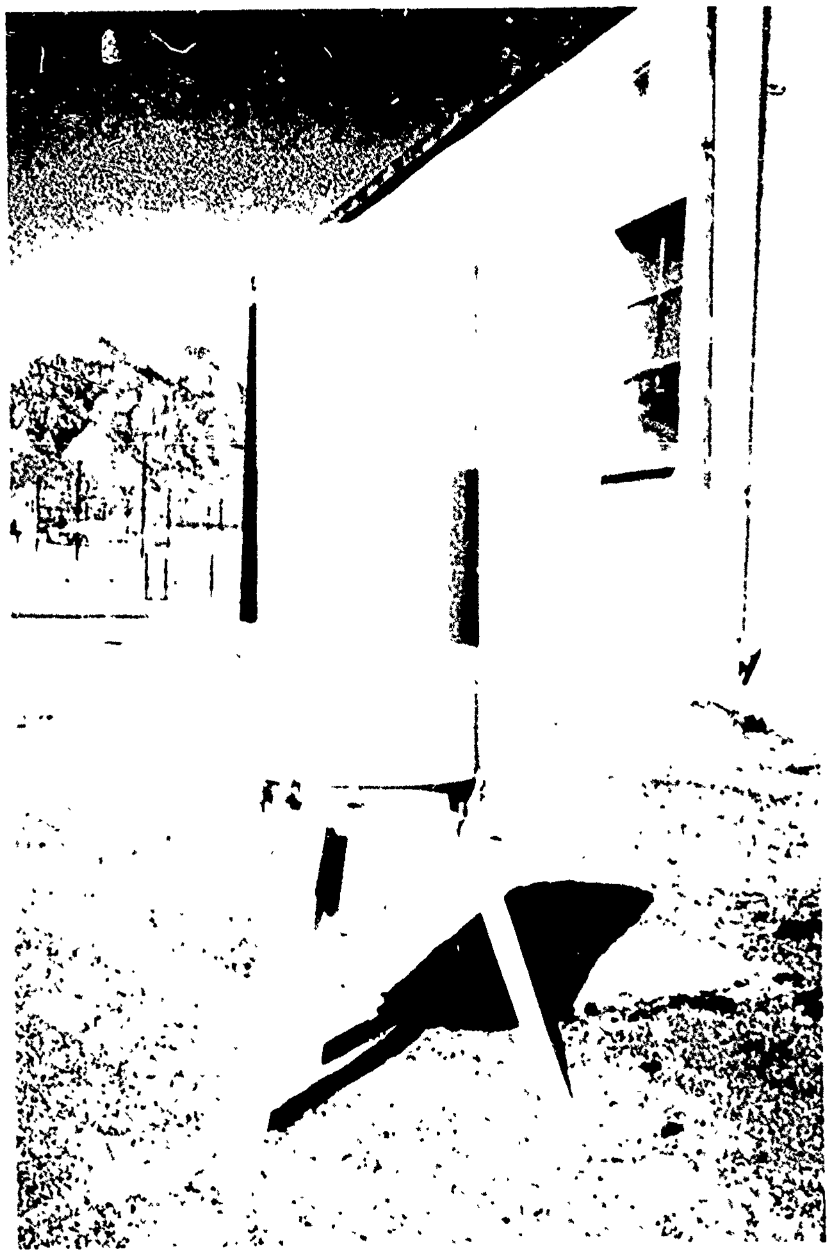

Figure 3. ASEA ceilometer.

AN/GVS-5 Laser Range Finder

The AN/GVS-5 is a lidar (Fig. 4). Its transmitter is a manually pulsed 20 millijoule per pulse Nd YAG laser (wavelength 1064 nanometers). It was designed to measure distances to solid targets located from 180 meters to 10 kilometers from the unit by measuring the time duration from pulse transmission to detection of the reflected energy from the target. The transmitter and receiver are located in a single unit. The unit is hand-held and battery operated. The operator places the eyepiece to his eye and orients the crosshairs on the target. He then presses the laser fire button and reads the distance to the target in meters, displayed digitally in the eyepiece. For the measurement of cloud bases, the observer aimed the AN/GVS-5 as nearly vertical as possible.

CLOUD-BASE HEIGHT MEASUREMENTS

Ranging Errors

Before the cloud-base height tests were conducted, the expected ranging errors were determined by providing a horizontal path for the transmitted beams and directing them to a solid target.

Ranging tests were conducted on the AN/GVS-5 laser range finder, the ASEA ceilometer, and the ceiloskop by using an M109-tactical van as a target (Fig. 5). The van was positioned at measured 152.5-meter intervals along a straight path to 915 meters. Six measurements were taken with each instrument at each 152.5-meter interval. These six measurements were averaged at each interval and the percent error between the average measurement of each instrument and the actual distance was calculated. The results of the ranging errors are shown in Table 1. Figure 6 shows a graph of the Impulsphysik ceiloskop, the AN/GVS-5, and the ASEA ceilometer ranging errors.

The large errors obtained for the ceiloskop can be attributed to the fact that the baseline (25 meters) is small compared to the actual range, and any error in reading the angle will result in a large measured range error. The expected ranging error can be obtained from [6]

$$\Delta R = 25 \, \mathrm{Sec}^2 \alpha \, \Delta \alpha$$

where α is the angle between the detector pointing direction and the baseline. This type of error is inherent in the bistatic technique.

Cloud-Base Height Measurements

Cloud-base heights were measured with the AN/GVS-5, the ceiloskop, the ASEA ceilometer, and the AN/GMQ-13A at Randolph Air Force Base, San

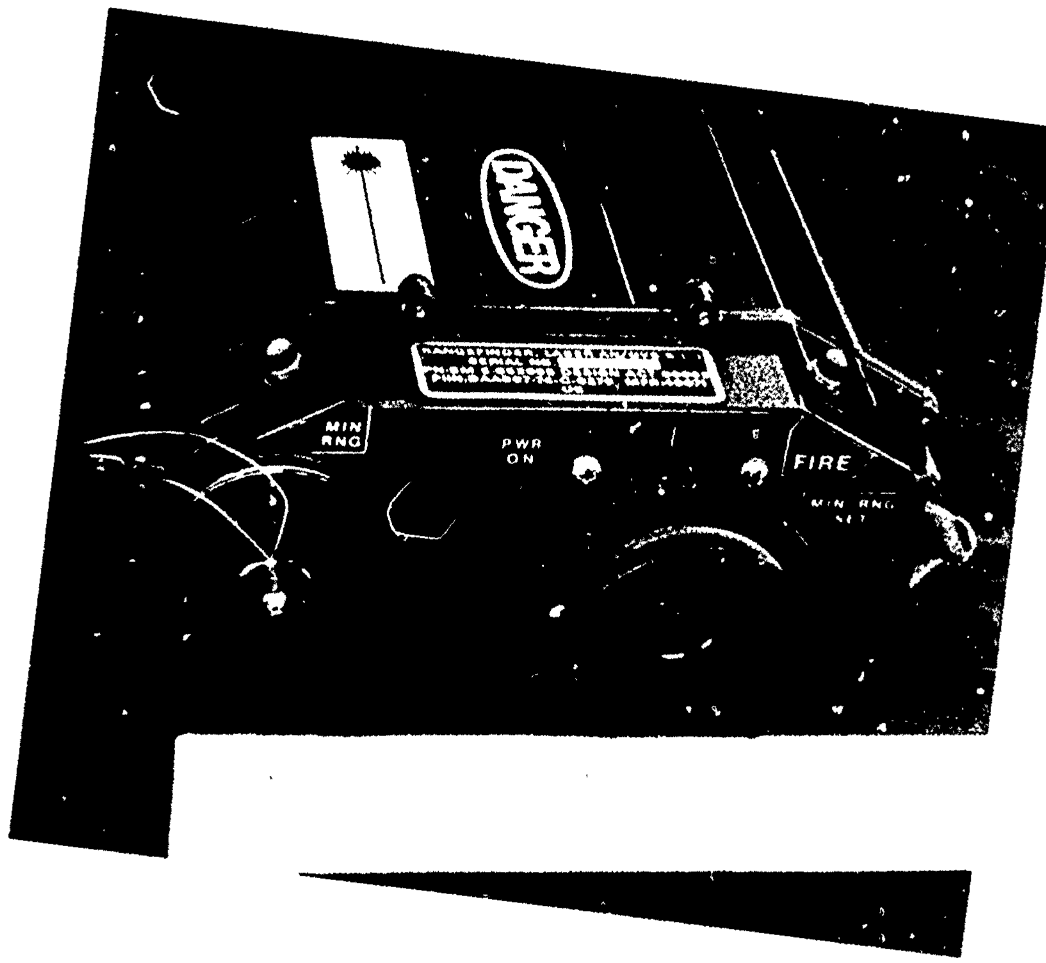

Figure 4. AN/GVS-5.

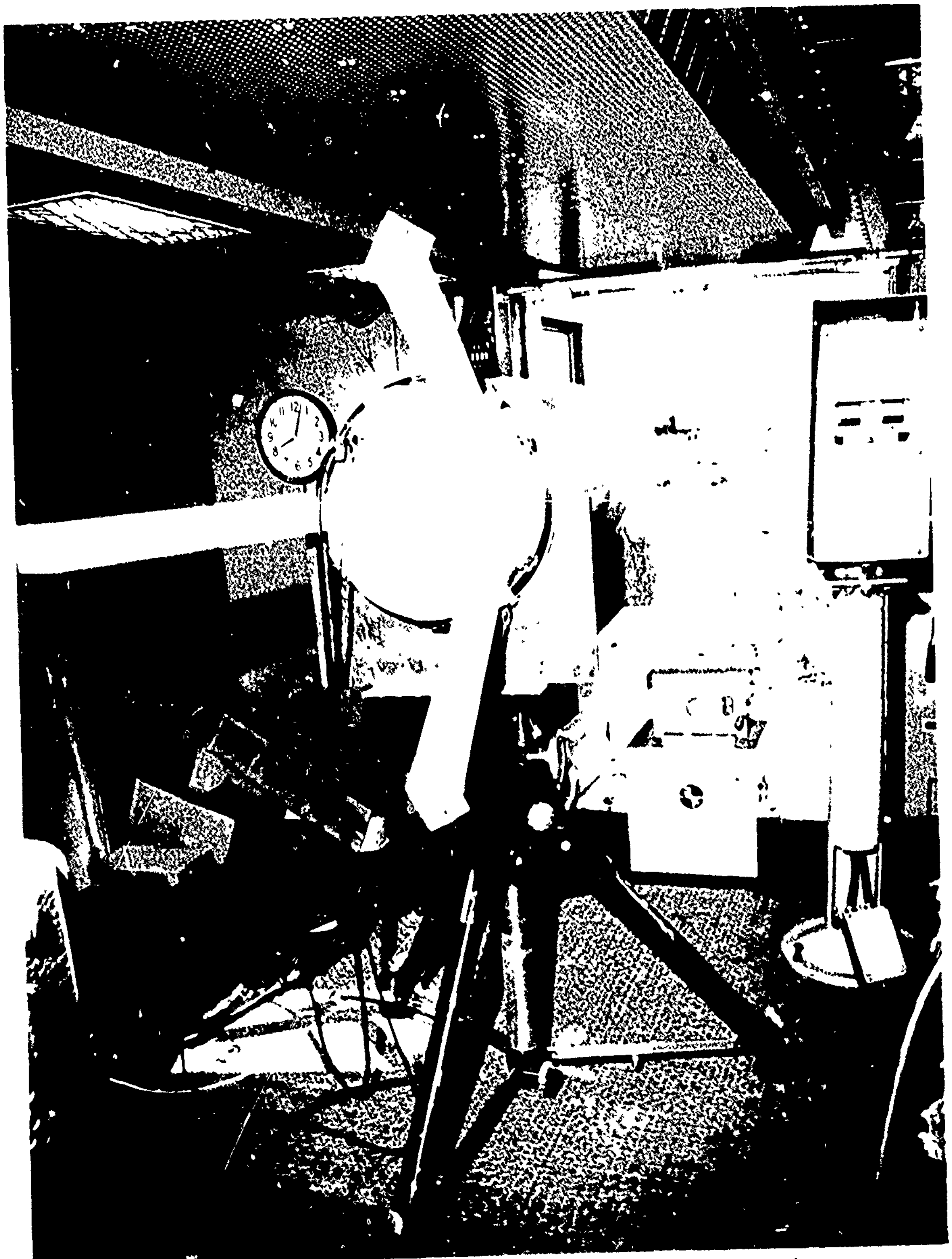

Figure 5. Photo of inside of data van showing target van in background.

TABLE 1

RANGING ERRORS

Instrument	Actual Distance (m)	Average Measured Distance (m)	Percent Error
AN/GVS-5	304.9	303.3	-0.51
	457.3	463.3	1.31
	609.8	613.3	0.57
	762.2	763.3	0.14
	914.6	920.0	0.59
	2000	2001.7	0.08
ASEA Ceilometer	155.2	160.1	3.2
	306.4	305.8	-0.2
	458.5	460.1	0.3
	611.0	602.4	-1.4
	763.1	765.5	0.3
	916.0	915.2	-0.09
Ceiloskop	153.0	152.7	-0.2
	305.5	307.3	0.6
	457.9	439.0	-4.1
	610.4	596.3	-2.3
	762.8	813.7	6.7
	915.2	1101.5	20.4

Estimated angle of inclination resolution = 0.25 degree.

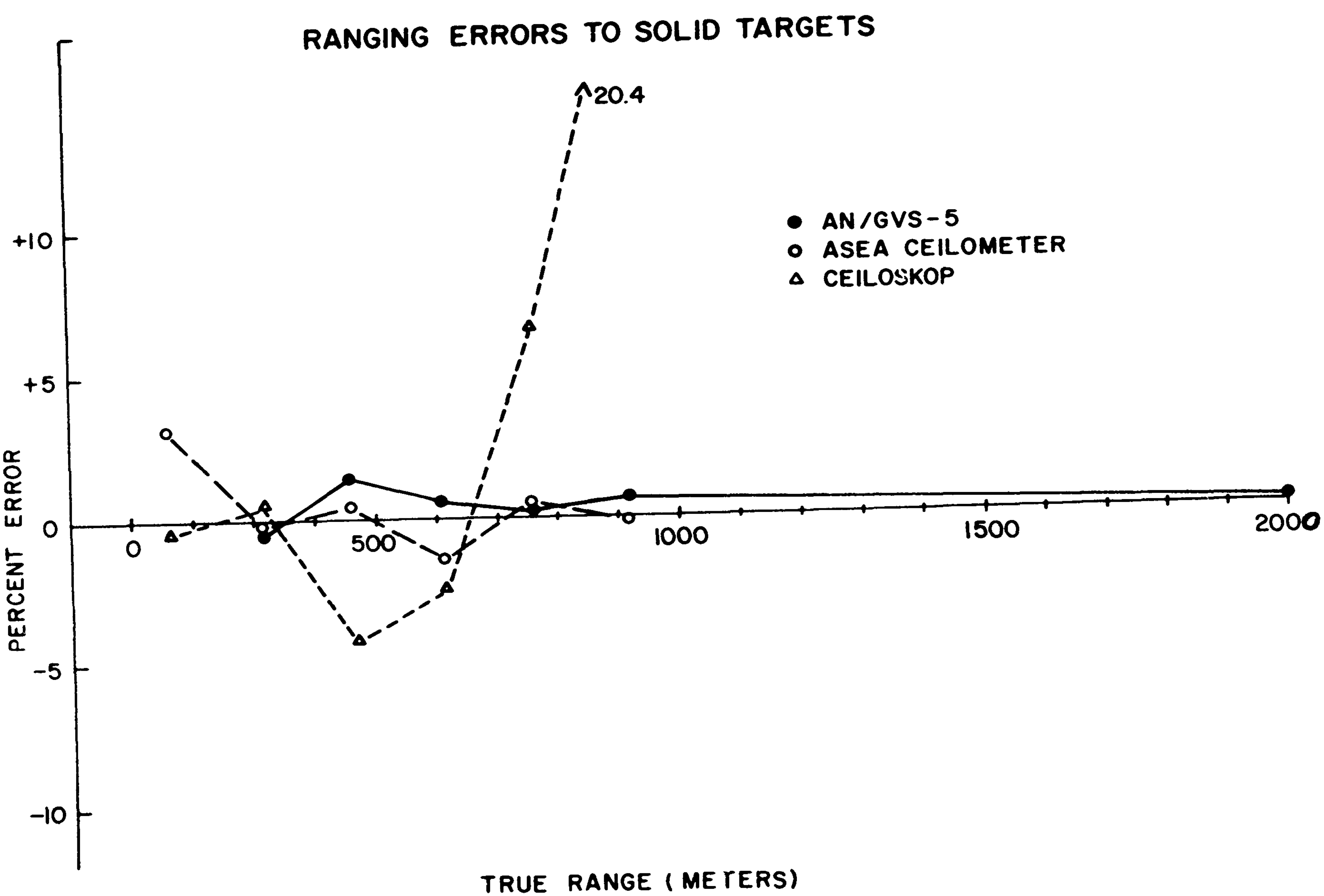

F·   6. Ranging errors of the AN/GVS-5, ASEA ceilometer, and ceiloskop.

Antonio, Texas, during November-December 1975. During these months, this station has a high occurrence of stratus clouds with bases which can be expected between 60 and 2000 meters in altitude.

Figure 7 is a sketch of the experimental setup geometry used. The ASEA ceilometer and ceiloskop projector were colocated at the rotating beam ceilometer detector. The instruments were leveled to provide a vertical transmitter beam. The AN/GVS-5 operator was approximately 10 meters from the RBC detector and was ranging vertically.

The procedure for collecting data from the RBC was to telephone the Air Weather Service observer on duty and get three readings (taps) from him on the RBC indicator. These readings were taken in as narrow a time frame as possible so that all measurements would have little time variation. Estimated time variation for all measurements was 4 minutes. The three RBC taps were averaged and that value was taken as the cloud-base height measurement for that hour. The procedure for collecting cloud height data with the AN/GVS-5 was to get three cloud height measurements while standing 10 meters away from the RBC detector and while aiming the AN/GVS-5 as nearly vertical as possible. These three measurements were then averaged to provide the hourly cloud height measurement for the AN/GVS-5.

The procedure for collecting cloud height data from the ASEA ceilometer was to choose the lower ends of three marks on the chart recorder as near to the other hourly readings as possible. These three values were then averaged to give the hourly cloud height measurement.

The procedure for obtaining cloud height data with the ceiloskop was to rotate the detector upward along the beam axis of the projector until the first modulated pulsing was detected from the backscatter of the cloud base. At this point the angle of inclination was noted and recorded. Then the detector was rotated farther upward until the modulated pulses ceased. At that point another angle of inclination was noted and recorded. Three of these types of readings were taken. The average angle of inclination for each sweep across the beam spot on the cloud base was calculated. These three average angles of inclination were then averaged to provide the angle of inclination used in the calculation of the cloud-base height for that hour.

The results of cloud height measurements are shown in Figs. 8 through 11. Figure 8 displays the resultant cloud-base height measurements obtained over a 28-hour period commencing at 0600 hours 28 November 1975. The morning hours, 0600 to 1100 hours, were dominated by fog. The results from the AN/GVS-5, with its minimum range of 180 meters, are not valid for this time interval. Clearing occurred at approximately 1200 hours; low-level stratus clouds entered the area at 2200 hours and remained through 1000 hours. During the latter period, the cloud-base height measurements showed the same general trends with the ceiloskop reading

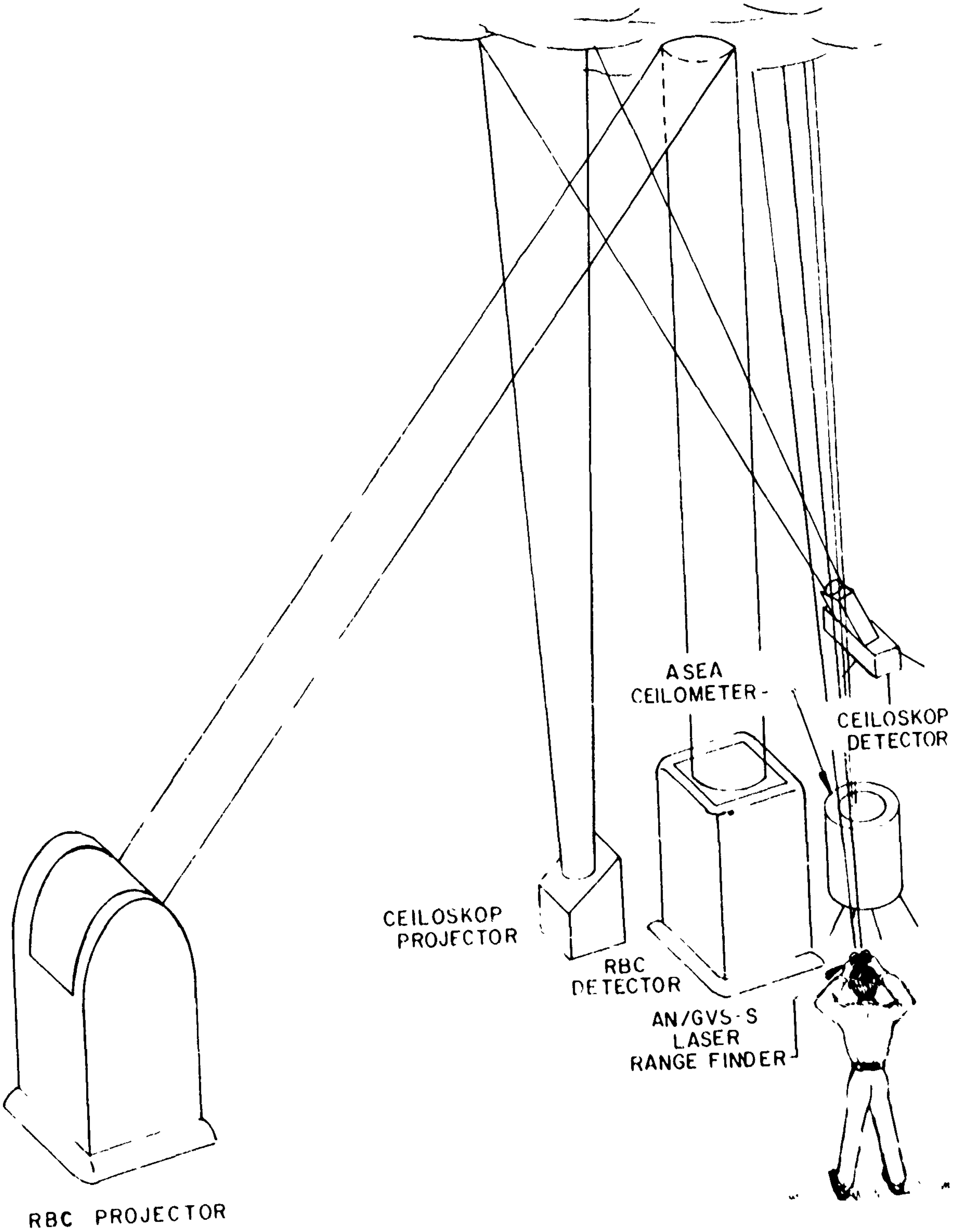

Figure 7. Diagram of equipment location geometry during comparison experiment.

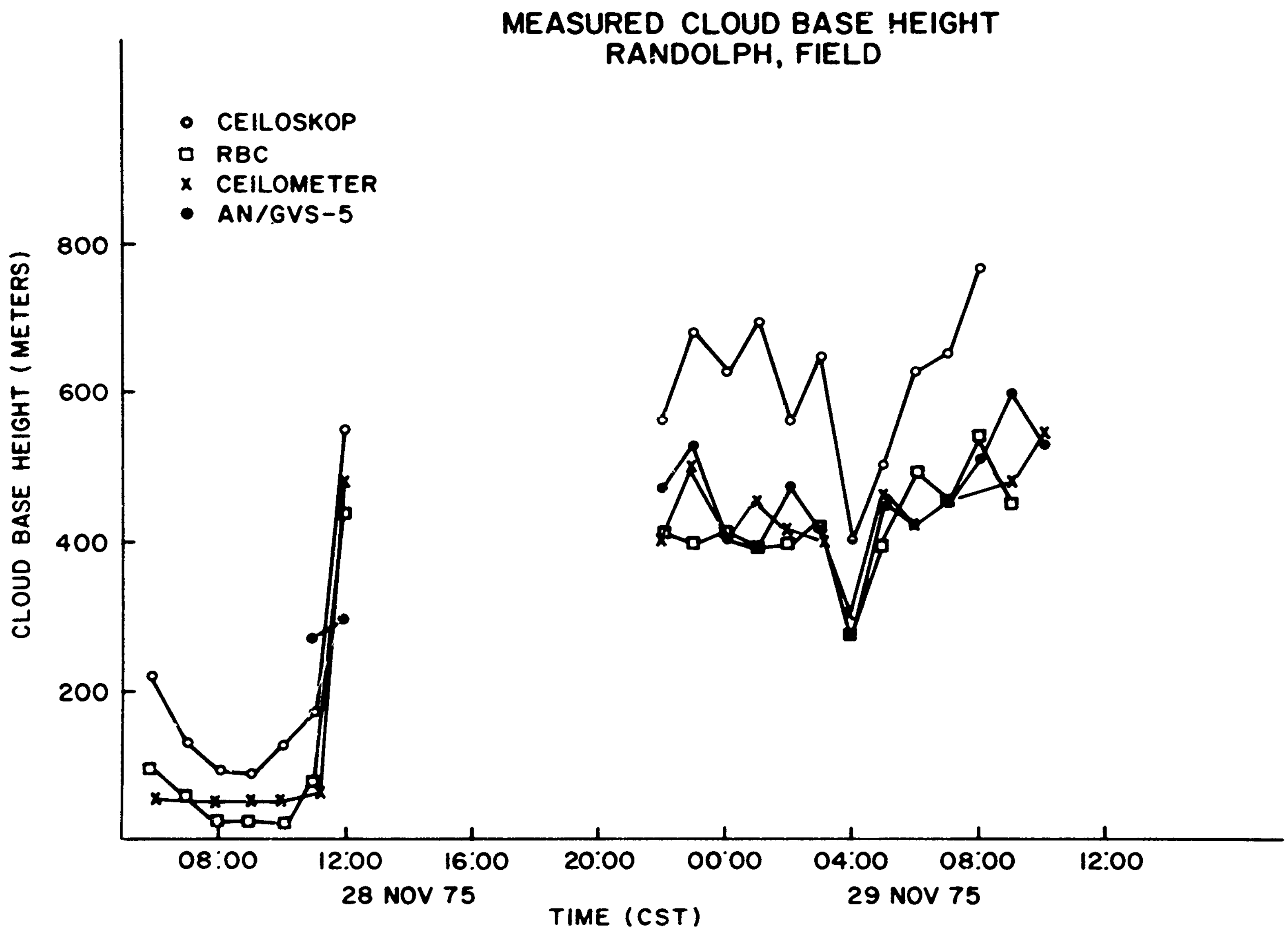

Figure 8. Cloud base height measurements 28-29 Nov 75.

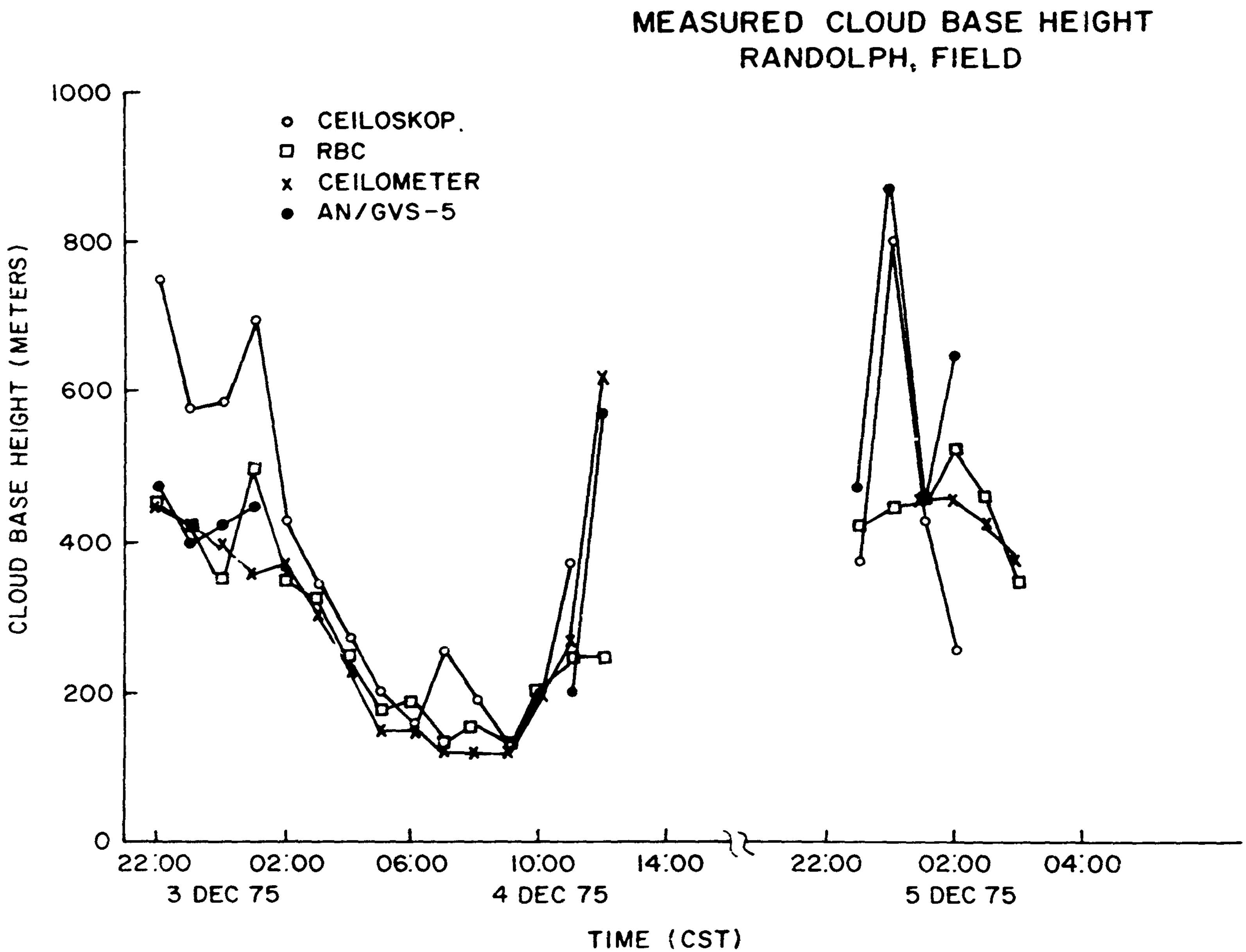

Figure 9. Cloud ˍase height measurements 3-5 Dec 75.

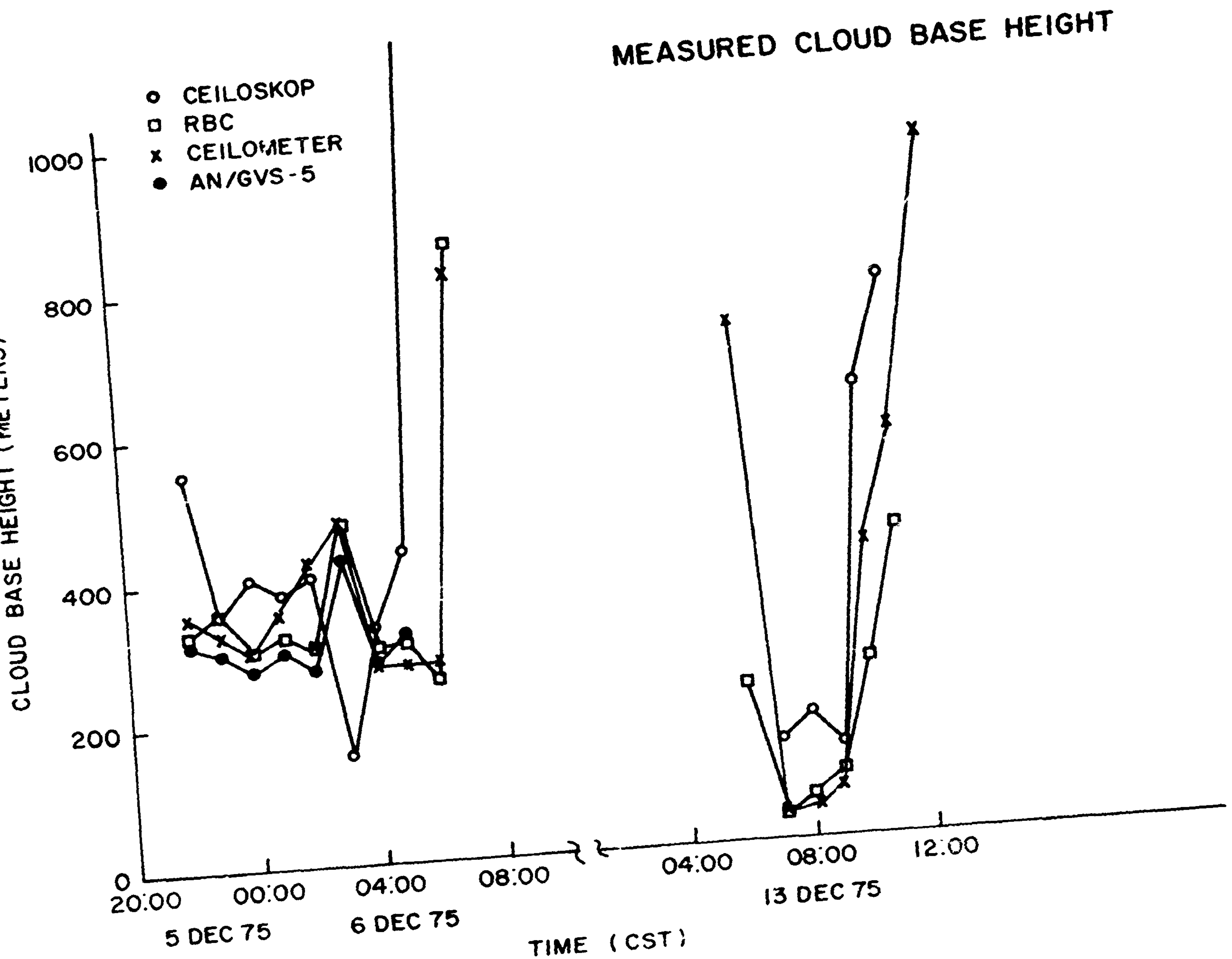

Figure 10. Cloud base height measurements 5, 6, 13 Dec 75.

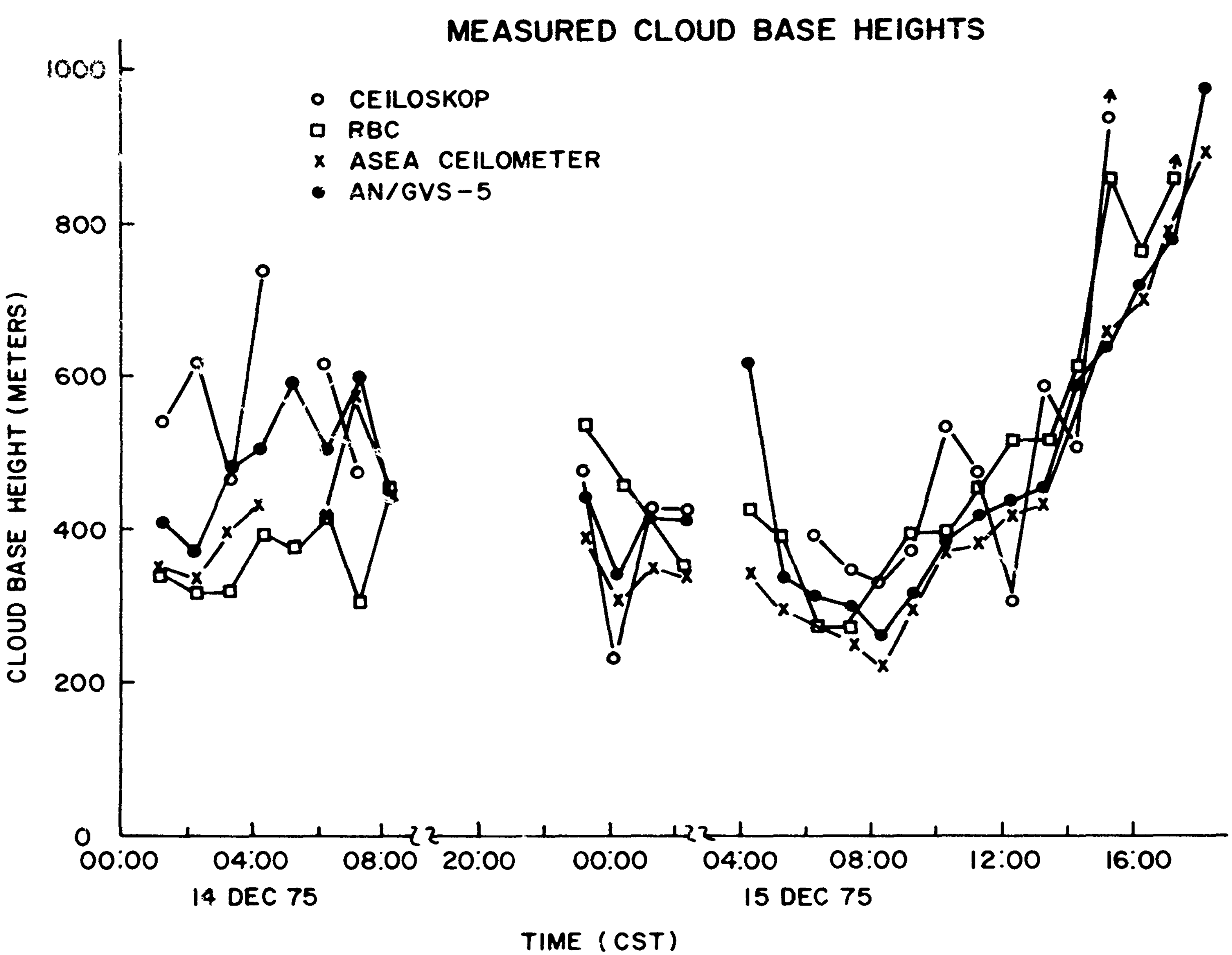

Figure 11. Cloud base height measurements 14-15 Dec 75.

consistently higher than the other instruments. This might have been due to an inherent error in the instrument caused by the short baseline.

Measured cloud-base heights for 3-5 December 1975 are shown in Fig. 9. As before, only the readings obtained from the AN/GVS-5 where the cloud height is above 180 meters are shown. Measured values of cloud-base heights for 5, 6, 13, 14, and 15 December are shown in Figs. 10 and 11.

Figures 8 through 11 show that the long-term trends for all instruments are the same. The heights obtained from the ceiloskop deviate rapidly from the results obtained from the other instruments and show more short-term variation about the longest trends. This difference could be attributed to the short baseline of the instrument.

The RBC, ASEA ceilometer, and AN/GVS-5 have more similar short-term characteristics. There are differences in the measured heights, and there does not seem to be a consistent pattern in these differences. This inconsistency may be due to spatial differences in equipment locations, differences in beam geometry, and small differences in sampling times which could not be avoided.

To show the similarity of the measured cloud-base heights obtained from the RBC, ASEA ceilometer and AN/GVS-5, the measurements from the various pairs were cross correlated. These results are presented in Table 2. The cross-correlated data over the entire data collection period from 28 November to 15 December 1975 are presented in Table 3 and graphically in Figs. 12 through 14. The appropriate formulas and variable definitions are given in Appendix B. Correlation data are summarized in Table 4 and Figs. 15, 16, and 17.

Data for the ceiloskop were not used in the scatter plots in the regression analysis. The values associated with the cloud heights obtained from this instrument seemed to vary more rapidly and were considerably higher than the heights obtained from other instruments. These differences were particularly true for ceilings above about 400 meters. Since the objective of the study was to evaluate the performance of the AN/GVS-5 as a cloud-base height indicator, performance of the ceiloskop was not determined beyond a qualitative analysis.

CONCLUSIONS

Correlation of the AN/GVS-5 with the AN/GMQ-13A rotating beam ceilometer indicates that it will effectively measure cloud heights above 180 meters. However, minimum range limitations of the AN/GVS-5 render it ineffective below 180 meters.

The correlation between the AN/GVS-5 and the ASEA ceilometer is much higher than the comparison to the rotating beam ceilometer. This indicates that the lidar technique is probably more sensitive to the backscatter medium than the triangulation method used by the rotating beam ceilometer.

These preliminary comparisons indicate that continued investigation of the methods to modify the cloud height measurements of the AN/GVS-5 is warranted.

With proper modifications, this instrument could make effective cloud height measurements from a mobile posture.

TABLE 2

LINEAR REGRESSION AND CORRELATION COEFFICIENTS FOR COMPARISON DATA

	28 - 29 November			3 - 4 December			4 - 5 December		
	n = 13	n = 12	n = 12	n = 7	n = 13	n = 6		n = 4	n = 3
	C vs G	R vs C	R vs G	C vs G	R vs C	R vs G	C vs G	R vs C	R vs G
a_0	41.68	159.63	68.11	73.75	-39.27	-47.71	Only 2	259.05	-402.89
a_1	1.01	0.60	0.92	0.90	0.92	1.10	valid	0.30	1.97
r^2	0.69	0.35	0.55	0.85	0.91	0.85	comparison	0.78	0.69
r	0.83	0.59	0.74	0.92	0.95	0.92	points	0.88	0.83
$\bar{x}$	x = 400	x = 435	x = 435	x = 374	x = 300	x = 300		x = 485	x = 465
$\bar{y}$	445.19	418.74	469.65	412.19	237.91	282.70		389.04	515.39
Sy.x	46.19	56.18	57.18	60.05	39.23	54.51		13.62	86.87
S_0	84.27	108.55	110.47	64.53	26.51	88.77		50.61	621.06
S_1	0.21	0.26	0.26	0.17	0.09	0.23		0.11	1.32

	5 - 6 December			13 December			14 December		
	n = 6	n = 7	n = 9	n = 4	n = 6	n = 2	n = 7	n = 6	n = 7
	C vs G	R vs C	R vs G	C vs G	R vs C	R vs G	C vs G	R vs C	R vs G
a_0	29.52	-39.04	-20.79	90.20	26.04	Only 2	101.30	140.81	294.18
a_1	0.97	0.99	0.98	0.93	1.59	valid	0.89	0.67	0.47
r^2	0.99	0.98	0.99	0.99	0.63	comparison	0.83	0.68	0.11
r	0.99	0.99	0.99	0.99	0.79	points	0.91	0.82	0.33
$\bar{x}$	x = 450	x = 550	x = 550	x = 450	x = 450		x = 450	x = 380	x = 380
$\bar{y}$	467.53	504.33	520.44	508.74	739.60		501.03	397.16	473.41
Sy.x	20.01	33.76	22.39	26.54	202.65		33.57	29.64	75.52
S_0	17.88	30.15	18.94	47.28	136.30		75.12	87.86	223.87
S_1	0.04	0.07	0.04	0.07	0.61		0.18	0.23	0.59

	14 - 15 December		
	n = 19	n = 18	n = 18
	C vs G	R vs C	R vs G
a_0	74.59	-27.49	74.92
a_1	0.93	0.88	0.76
r^2	0.90	0.92	0.78
r	0.95	0.96	0.88
$\bar{x}$	x = 560	x = 630	x = 630
$\bar{y}$	597.32	526.80	554.96
Sy.x	60.40	47.24	71.67
S_0	35.27	34.48	52.31
S_1	0.07	0.07	0.10

C = ASEA ceilometer
G = AN/GVS-5
R = RBC
n = Number of valid comparisons

See Appendix B for explanation of terms.

TABLE 3

TOTAL LINEAR REGRESSION AND CORRELATION COEFFICIENTS FOR COMPARISON DATA
(28 Nov - 15 Dec 75)

	GVS-5 vs ASEA n = 61	GVS-5 vs RBC n = 63	ASEA vs RBC n = 73
m	0.92	0.81	0.91
b	-8.77	68.17	61.75
S'_x	159.92	129.58	157.71
S'_y	170.54	132.74	161.65
r_{xy}	0.91	0.77	0.89
$\hat{r}$	0.89	0.60	0.80
S'_{xy}	24,939.11	13,165.23	22,706.22

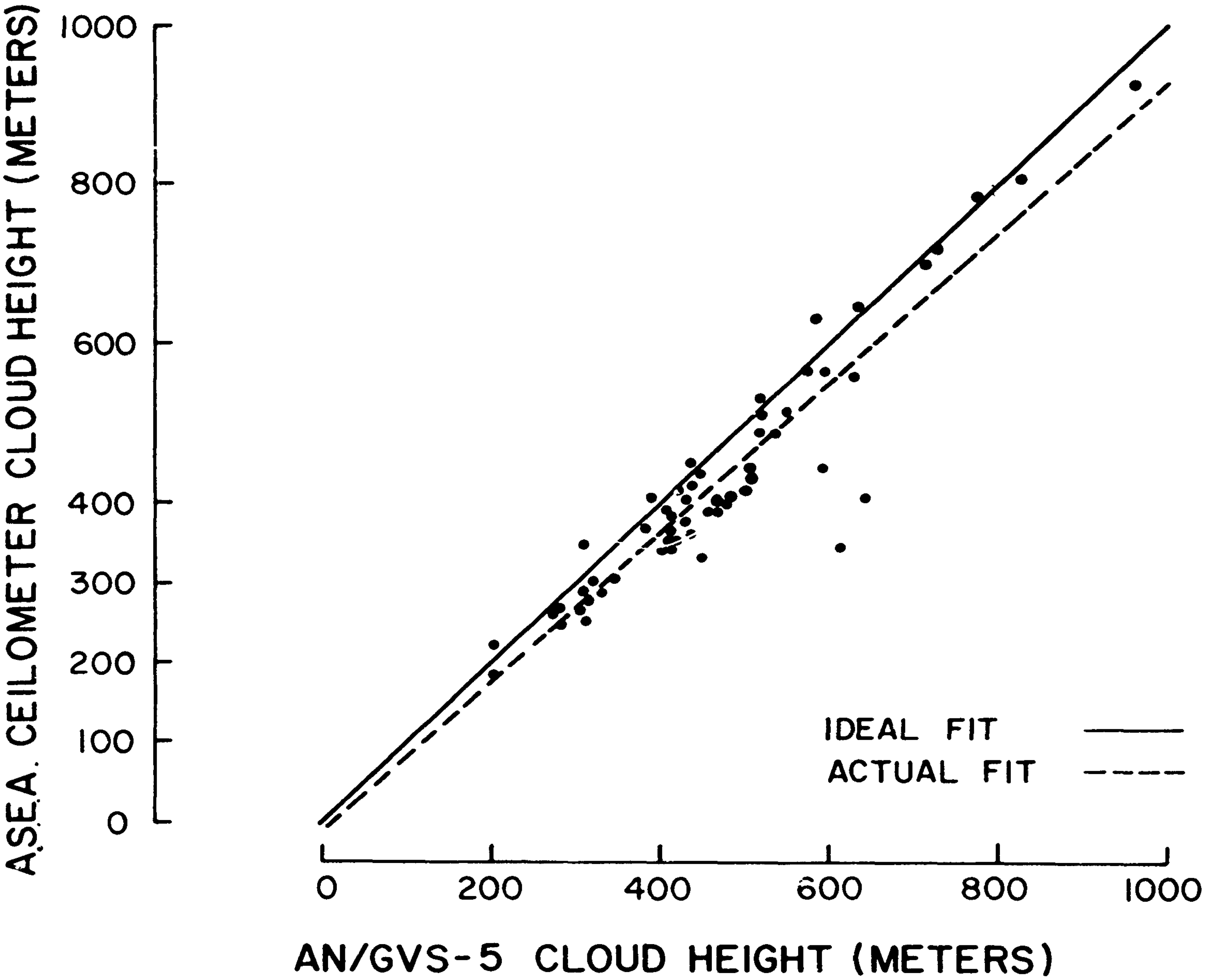

Figure 12. Scatter diagram of AN/GVS-5 vs. ceilometer.

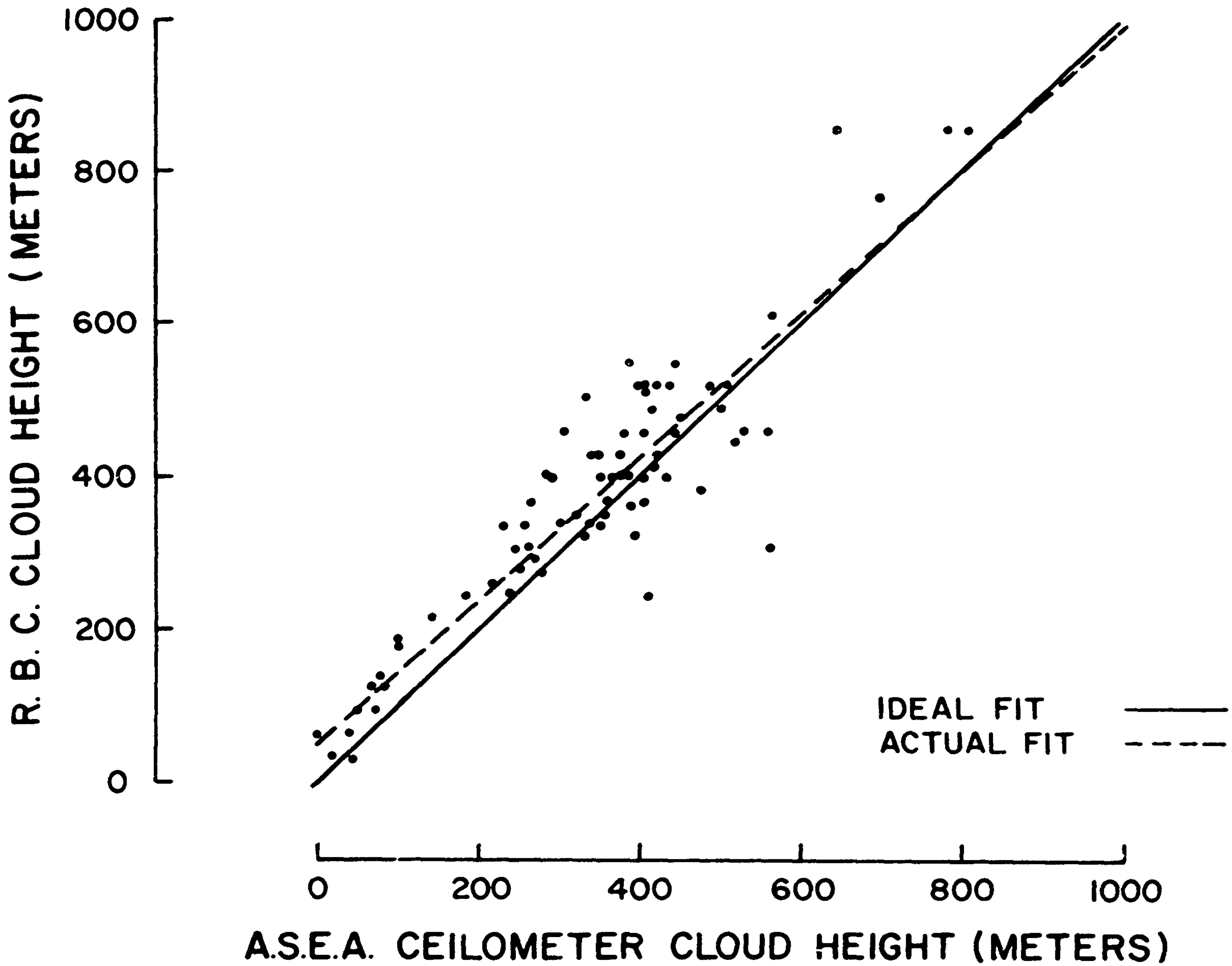

Figure 13. Scatter diagram of ceilometer vs. RBC.

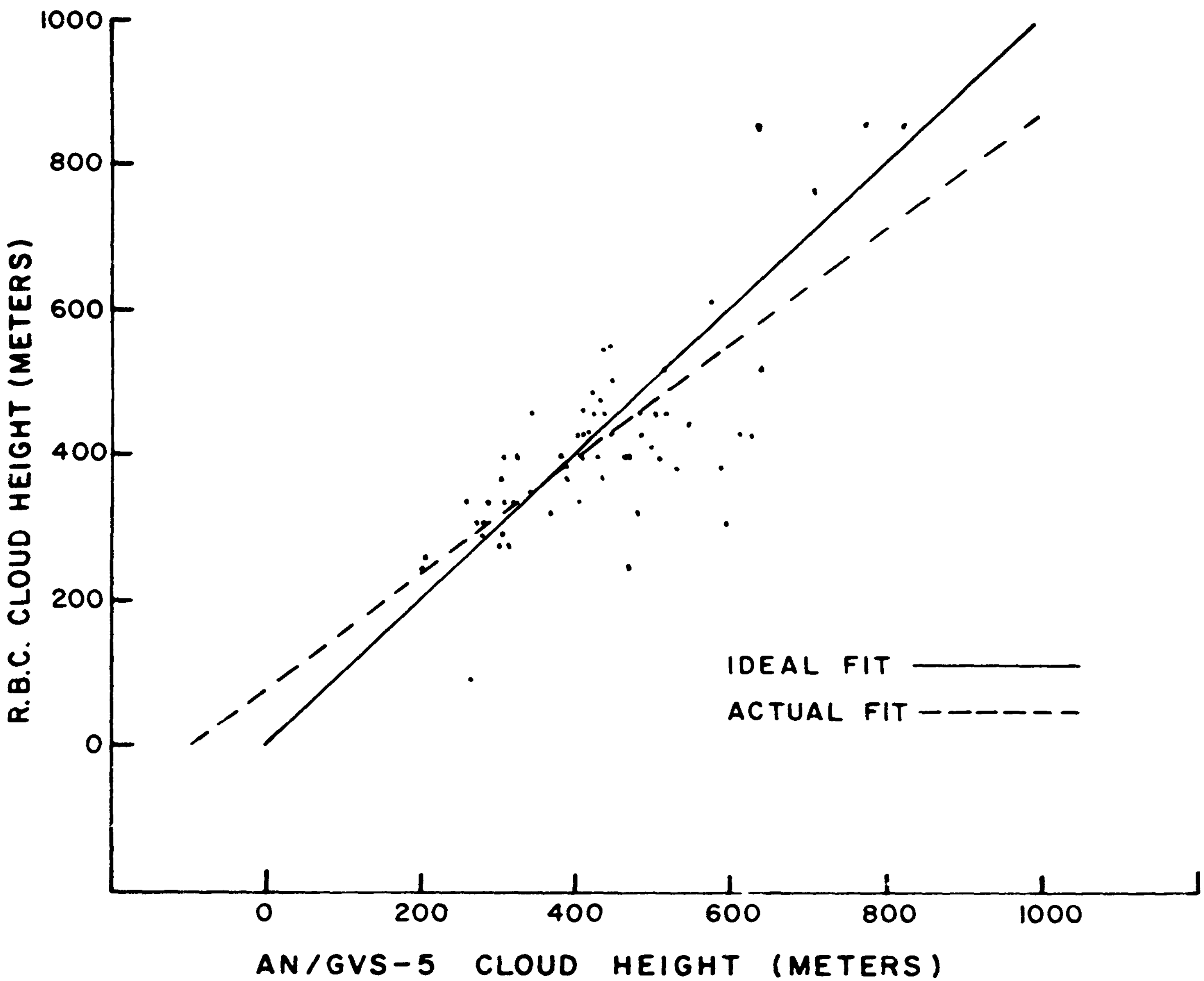

Figure 14. Scatter Diagram of AN/GVS-5 vs. RBC.

TABLE 4

PERCENTAGE OF TOTAL DATA GROUP COMPARISONS IN WHICH THE CORRELATION COEFFICIENT WAS ABOVE THE INDICATED VALUE

Correlation Coefficient	ASEA Ceilometer vs AN/GVS-5 (n = 56)(%)	RBC vs ASEA Ceilometer (n = 66)(%)	RBC vs AN/GVS-5 (n = 55)(%)
0.90	83.3	42.9	33.3
0.80	16.7	28.6	33.3
0.70	-	14.3	16.7
0.60	-	-	-
0.50	-	14.2	-
0.40	-	-	-
0.30	-	-	16.7

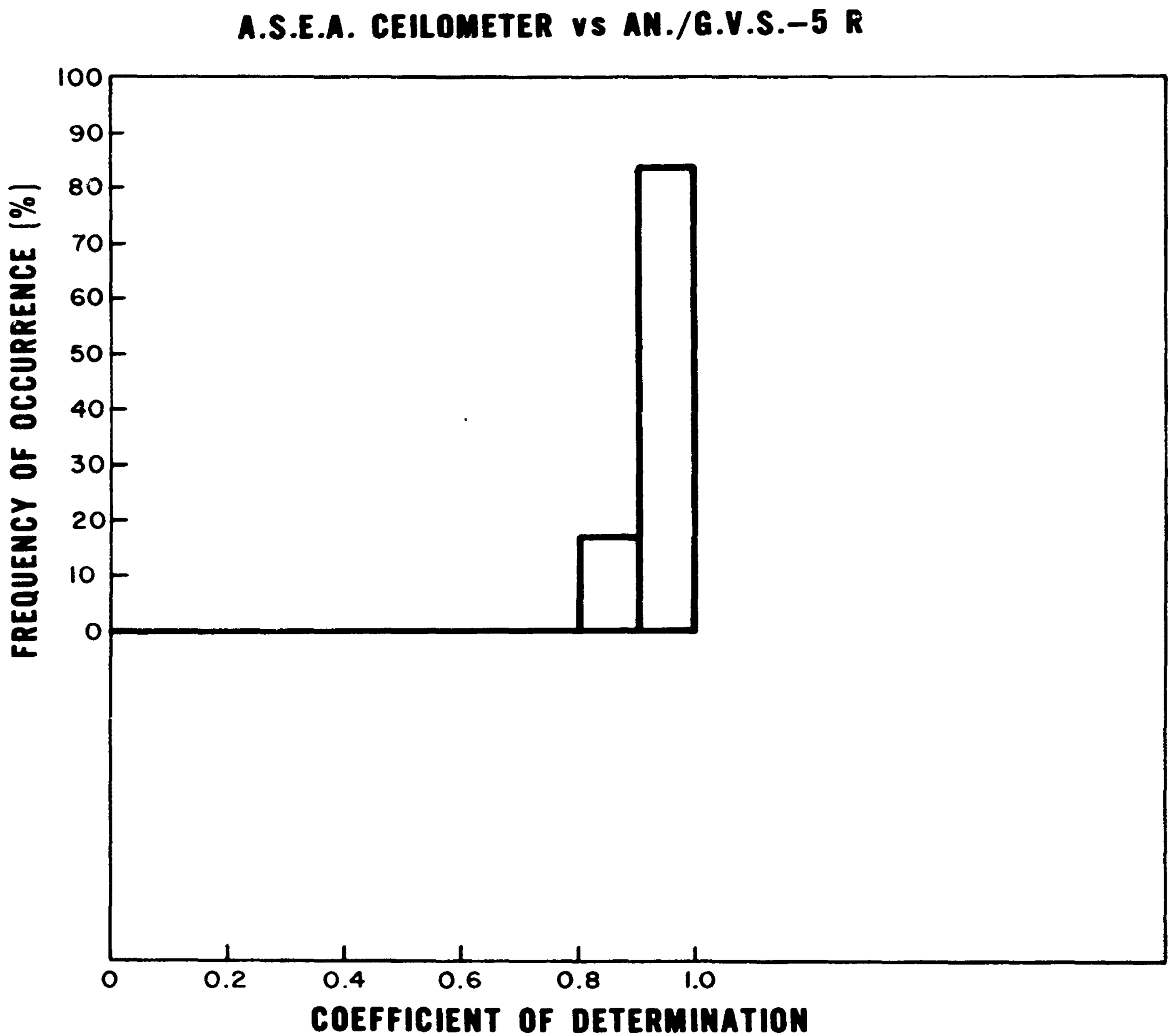

Figure 15. Bar graph of frequency of occurrence of coefficients of determination for AN/GVS-5 vs ceilometer.

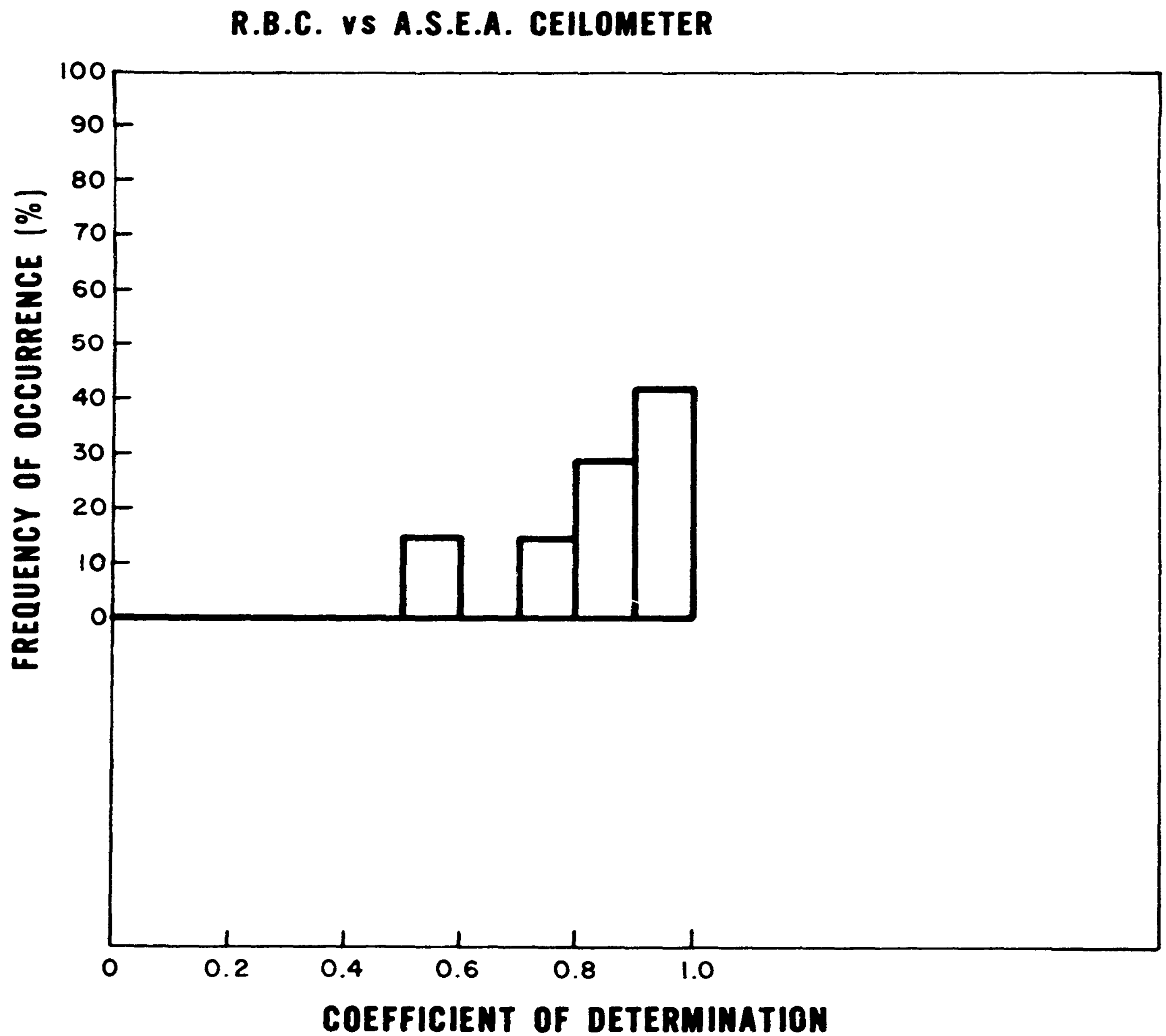

Figure 16. Bar graph of frequency of occurrence of coefficients of determination for ceilometer vs. RBC.

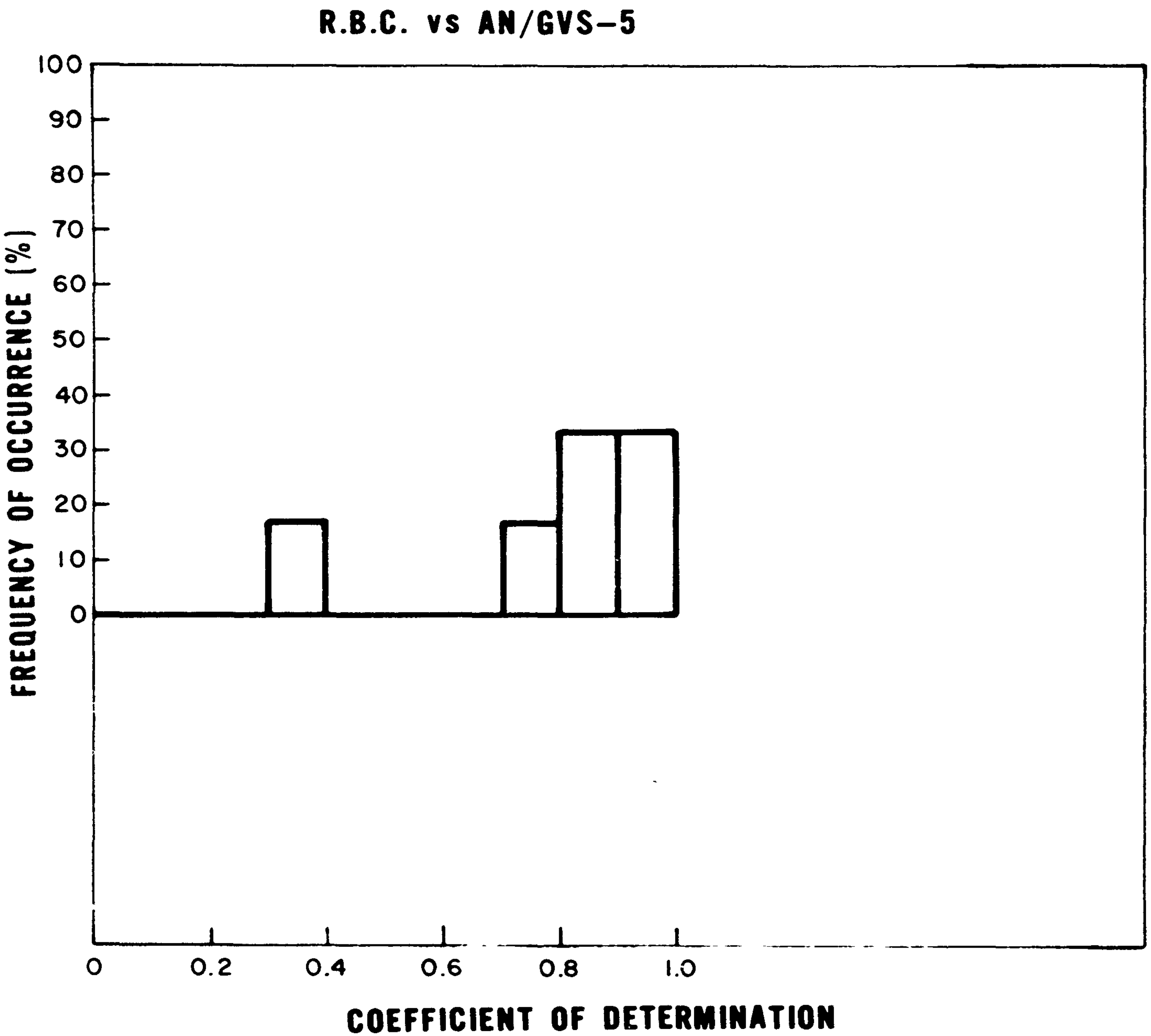

Figure 17. Frequency of occurrence of coefficients of determination for AN/GVS-5 vs. RBC.

REFERENCES

1. Cloud Height Set, AN/GMQ-13A (1967) To. 31M1-2GMQ13-12.

2. Cloud Height Set, AN/TMQ-25 AWSP 105-3, July 1971.

3. Collis, T. H. R., "Lidar Observation of Cloud," Science, 49, 978.

4. George, D. H. "A New Lidar Ceilometer for Airfield Operations," Proceeding Sixth International Conference on Aerospace and Aeronautical Meteorology, November 1974, p 464.

5. Moroz, E. Y., C. L. Lawrance, and G. A. Travers, "Laser Ceilometer," AFCRL-TR-73-0751, December 1973.

6. George, D. H. "Precision and Representativeness of Ceilometer Cloud Height Measurements in the Runway Approach Area," Proceeding Fifth International Conference on Aerospace and Aeronautical Meteorology, 22-26 May 1972.

APPENDIX A

EQUIPMENT SPECIFICATIONS

AN/GMQ-13A Rotating Beam Ceilometer

1. Source - incandescent sealed beam lamps
2. Source modulation frequency - 120 hertz
3. Detector - silicone avalanche photodiode
4. Baseline - 152 meters
5. Beam rotation rate 3 second per 180 degrees
6. Baseline check duration 3 seconds
7. Measurement accuracy - 20 percent error at 10 times the baseline
8. Power requirements - 117 volts alternating current, 1 kilowatt

AN/GVS-5 Laser Rangefinder

1. Source - 20 millijoule per pulse, Nd YAG laser, manually pulsed, wavelength 1064 nanometers, pulsewidth 7 nanoseconds, beam divergence 4 milliradians, beam exit diameter = 7 millimeters
2. Detector - silicone avalanche photodiode, 150Å bandwidth optical filter, divergence 1 milliradian
3. Maximum firing rate - 6 per minute
4. Range 180 meters to 10 kilometers, range gate in 10-meter intervals
5. Power requirements - 28 volts direct current battery type BB-516 ()/U (fully charged battery will be adequate for 200 to 500 rangings)

ASEA Ceilometer

1. Source - 25 watt per pulse GaAs diode array laser. Wavelength 906.0 nanometers, pulse repetition frequency 2 kilohertz, pulsewidth 50 nanoseconds, beam divergence 2 milliradians

2. Detector - silicone avalanche photodiode. Band-pass filter width 12.0 nanometers, field of view divergence 2 milliradians.

3. Measurement range 10 to 1000 meters, range gate in 5-meter intervals.

4. Power requirements - 115 volts, 60 hertz, 330 watts for the transceiver unit; 115 volts, 60 hertz, 15 watts for the recorder.

5. Measurement interval 75 seconds.

6. Measurement duration 30 seconds.

Impulsphysik Ceiloskop

1. Source - xenon flash lamp, flash rate 3 per second emergent beam diameter = 24 centimeters, beam divergence = 3.68 degrees.

2. Detector - silicone avalanche photodiode

3. Power requirements - 12 volts direct current battery, automatic deactivate on detector and electronics after 90 to 105 seconds running time. Approximately 30 hours continuous operation on a fully charged battery pack.

APPENDIX B

CALCULATIONS OF LINEAR REGRESSION AND CORRELATION COEFFICIENTS FOR COMPARISON DATA

Sums for Two Variables to fit a straight line

$$y = a_0 + a_1 x \text{ for a set of data points}$$

$$\{(x_i, y_i),\ i = 1, 2, ---, n\} \quad \text{where } n > 2$$

regression coefficients a_0, a_1

$$a_0 = \bar{y} - a_1 \bar{x}$$

$$a_i = \frac{x_i y_i - \dfrac{\Sigma x_i \, \Sigma y_i}{n}}{\Sigma x_i^2 - \dfrac{(\Sigma x_i)^2}{n}}$$

Coefficient of determination

$$r^2 = \frac{\left[\Sigma x_i y_i - \dfrac{\Sigma x_i \, \Sigma y_i}{n}\right]^2}{\left[\Sigma x_i^2 - \dfrac{(\Sigma x_i)^2}{n}\right]\left[\Sigma y_i^2 - \dfrac{(\Sigma y_i)^2}{n}\right]}$$

r^2 is the proportion of variation about the mean $\bar{y}$ explained by the regression where $0 \leq r^2 \leq 1$; and if $r^2 = 1$, the regression line fits perfectly.

Correlation Coefficient

$$r = \frac{\left[\Sigma x_i y_i - \dfrac{\Sigma x_i \, \Sigma y_i}{n}\right]}{\left\{\left[\Sigma x_i^2 - \dfrac{(\Sigma x_i)^2}{n}\right]\left[\Sigma y_i^2 - \dfrac{(\Sigma y_i)^2}{n}\right]\right\}^{\frac{1}{2}}}$$

The estimated value $\hat{y}$ on the regression line for any given x is

$$\hat{y} = a_0 + a_1 x$$

The standard error of estimate of $\hat{y}$ on x is

$$S_{y \cdot x} = \left[\frac{\Sigma\ (y_i - \hat{y}_i)^2}{n - 2}\right]^{\frac{1}{2}}$$

$$= \left[\frac{\Sigma\ y_i^2 - a_0\ \Sigma\ y_i - a_1\ \Sigma\ x_i\ y_i}{n - 2}\right]^{\frac{1}{2}}$$

The standard error of the regression coefficient a_0 is

$$S_0 = S_{y \cdot x}\left[\frac{\Sigma\ x_i^2}{n\left[\Sigma\ x_i^2 - \frac{(\Sigma x_i)^2}{n}\right]}\right]^{\frac{1}{2}}$$

The standard error of the regression coefficient a_1 is

$$S_1 = \frac{S_{y \cdot x}}{\left[\Sigma\ x_i^2 - \frac{(\Sigma x_i)^2}{n}\right]^{\frac{1}{2}}}$$

For n comparisons of x and y;

$$\text{Slope (m)} = \frac{\frac{\Sigma x \Sigma y}{n} - \Sigma xy}{\frac{(\Sigma x)^2}{n} - \Sigma x^2}$$

$$\text{Intercept (b)} = \frac{\Sigma y - m\Sigma x}{n}$$

Coefficient of determination:

$$r^2 = \frac{m\left(\frac{\Sigma x \Sigma y}{n} - \Sigma xy\right)}{\left(\Sigma y^2 - \frac{(\Sigma y)^2}{n}\right)}$$

Standard deviation of x by n method:

$$S'_x = \left(\frac{\sum_{i=1}^{n} x_i^2 - n\,\overline{x^2}}{n}\right)^{1/2}$$

Standard deviation of y by n method:

$$S'_y = \left(\frac{\sum_{i=1}^{n} y_i^2 - n\,\overline{y^2}}{n}\right)^{1/2}$$

Covariance of x and y by n method:

$$S'_{xy} = \frac{1}{n}\left[\sum_{i=1}^{n} x_i y_i - \frac{1}{n}\sum_{i=1}^{n} x_i \sum_{i=1}^{n} y_i\right]$$

Correlation coefficient of x and y:

$$r_{xy} = \frac{S'_{xy}}{S'_x S'_y}$$

ATMOSPHERIC SCIENCES RESEARCH PAPERS

1. Lindberg, J.D., "An Improvement to a Method for Measuring the Absorption Coefficient of Atmospheric Dust and other Strongly Absorbing Powders," ECOM-5565, July 1975.
2. Avara, Elton, P., "Mesoscale Wind Shears Derived from Thermal Winds," ECOM-5566, July 1975.
3. Gomez, Richard B. and Joseph H. Pierluissi, "Incomplete Gamma Function Approximation for King's Strong-Line Transmittance Model," ECOM-5567, July 1975.
4. Blanco, A.J. and B.F. Engebos, "Ballistic Wind Weighting Functions for Tank Projectiles," ECOM-5568, August 1975.
5. Taylor, Fredrick J., Jack Smith, and Thomas H. Pries, "Crosswind Measurements through Pattern Recognition Techniques," ECOM-5569, July 1975.
6. Walters, D.L., "Crosswind Weighting Functions for Direct-Fire Projectiles," ECOM-5570, August 1975.
7. Duncan, Louis D., "An Improved Algorithm for the Iterated Minimal Information Solution for Remote Sounding of Temperature," ECOM-5571, August 1975.
8. Robbiani, Raymond L., "Tactical Field Demonstration of Mobile Weather Radar Set AN/TPS-41 at Fort Rucker, Alabama," ECOM-5572, August 1975.
9. Miers, B., G. Blackman, D. Langer, and N. Lorimier, "Analysis of SMS/GOES Film Data," ECOM-5573, September 1975.
10. Manquero, Carlos, Louis Duncan, and Rufus Bruce, "An Indication from Satellite Measurements of Atmospheric CO_2 Variability," ECOM-5574, September 1975.
11. Petracca, Carmine and James D. Lindberg, "Installation and Operation of an Atmospheric Particulate Collector," ECOM-5575, September 1975.
12. Avara, Elton P. and George Alexander, "Empirical Investigation of Three Iterative Methods for Inverting the Radiative Transfer Equation," ECOM-5576, October 1975.
13. Alexander, George D., "A Digital Data Acquisition Interface for the SMS Direct Readout Ground Station—Concept and Preliminary Design," ECOM-5577, October 1975.
14. Cantor, Israel, "Enhancement of Point Source Thermal Radiation Under Clouds in a Nonattenuating Medium," ECOM-5578, October 1975.
15. Norton, Colburn and Glenn Hoidale, "The Diurnal Variation of Mixing Height by Month over White Sands Missile Range, NM," ECOM-5579, November 1975.
16. Avara, Elton P., "On the Spectrum Analysis of Binary Data," ECOM-5580, November 1975.
17. Taylor, Fredrick J., Thomas H. Pries, and Chao-Huan Huang, "Optimal Wind Velocity Estimation," ECOM-5581, December 1975.
18. Avara, Elton P., "Some Effects of Autocorrelated and Cross-Correlated Noise on the Analysis of Variance," ECOM-5582, December 1975.
19. Gillespie, Patti S., R.L. Armstrong, and Kenneth O. White, "The Spectral Characteristics and Atmospheric CO_2 Absorption of the Ho^{+3}:YLF Laser at 2.05μm," ECOM-5583, December 1975.
20. Novlan, David J., "An Empirical Method of Forecasting Thunderstorms for the White Sands Missile Range," ECOM-5584, February 1976.
21. Avara, Elton P., "Randomization Effects in Hypothesis Testing with Autocorrelated Noise," ECOM-5585, February 1976.
22. Watkins, Wendell R., "Improvements in Long Path Absorption Cell Measurement," ECOM-5586, March 1976.
23. Thomas, Joe, George D. Alexander, and Marvin Dubbin, "SATTEL — An Army Dedicated Meteorological Telemetry System," ECOM-5587, March 1976.
24. Kennedy, Bruce W. and Delbert Bynum, "Army User Test Program for the RDT&E-XM-75 Meteorological Rocket," ECOM-5588, April 1976.

25. Barnett, Kenneth M., "A Description of the Artillery Meteorological Comparisons at White Sands Missile Range, October 1974 — December 1974 ('PASS' — Prototype Artillery [Meteorological] Subsystem)," ECOM-5589, April 1976.
26. Miller, Walter B., "Preliminary Analysis of Fall-of-Shot From Project 'PASS'," ECOM-5590, April 1976.
27. Avara, Elton P., "Error Analysis of Minimum Information and Smith's Direct Methods for Inverting the Radiative Transfer Equation," ECOM-5591, April 1976.
28. Yee, Young P., James D. Horn, and George Alexander, "Synoptic Thermal Wind Calculations from Radiosonde Observations Over the Southwestern United States," ECOM-5592, May 1976.
29. Duncan, Louis D. and Mary Ann Seagraves, "Applications of Empirical Corrections to NOAA-4 VTPR Observations," ECOM-5593, May 1976.
30. Miers, Bruce T. and Steve Weaver, "Applications of Meterological Satellite Data to Weather Sensitive Army Operations," ECOM-5594, May 1976.
31. Sharenow, Moses, "Redesign and Improvement of Balloon ML-566," ECOM-5595, June 1976.
32. Hansen, Frank V., "The Depth of the Surface Boundary Layer," ECOM-5596, June 1976.
33. Pinnick, R.G. and E.B. Stenmark, "Response Calculations for a Commercial Light-Scattering Aerosol Counter," ECOM-5597, July 1976.
34. Mason, J. and G.B. Hoidale, "Visibility as an Estimator of Infrared Transmittance," ECOM-5598, July 1976.
35. Bruce, Rufus E., Louis D. Duncan, and Joseph H. Pierluissi, "Experimental Study of the Relationship Between Radiosonde Temperatures and Radiometric-Area Temperatures," ECOM-5599, August 1976.
36. Duncan, Louis D., "Stratospheric Wind Shear Computed from Satellite Thermal Sounder Measurements," ECOM-5800, September 1976.
37. Taylor, F., P. Mohan, P. Joseph and T. Pries, "An All Digital Automated Wind Measurement System," ECOM-5801, September 1976.
38. Bruce, Charles, "Development of Spectrophones for CW and Pulsed Radiation Sources," ECOM-5802, September 1976.
39. Duncan, Louis D. and Mary Ann Seagraves, "Another Method for Estimating Clear Column Radiances," ECOM-5803, October 1976.
40. Blanco, Abel J. and Larry E. Traylor, "Artillery Meteorological Analysis of Project Pass," ECOM-5804, October 1976.
41. Miller, Walter and Bernard Engebos, "A Mathematical Structure for Refinement of Sound Ranging Estimates," ECOM-5805, November, 1976.
42. Gillespie, James B. and James D. Lindberg, "A Method to Obtain Diffuse Reflectance Measurements from 1.0 to 3.0μm Using a Cary 171 Spectrophotometer," ECOM-5806, November 1976.
43. Rubio, Roberto and Robert O. Olsen, "A Study of the Effects of Temperature Variations on Radio Wave Absorption," ECOM-5807, November 1976.
44. Ballard, Harold N., "Temperature Measurements in the Stratosphere from Balloon-Borne Instrument Platforms, 1968-1975," ECOM-5808, December, 1976.
45. Monahan, H.H., "An Approach to the Short-Range Prediction of Early Morning Radiation Fog," ECOM-5809, January 1977.
46. Engebos, Bernard Francis, "Introduction to Multiple State Multiple Action Decision Theory and Its Relation to Mixing Structures," ECOM-5810, January 1977.
47. Low, Richard D.H., Effects of Cloud Particles on Remote Sensing from Space in the 10-Micrometer Infrared Region, ECOM-5811, January 1977.
48. Bonner, Robert S. and R. Newton, "Application of the AN/GVS-5 Laser Rangefinder to Cloud Base Height Measurements," ECOM-5812, February 1977.

DISTRIBUTION LIST

Commanding Officer
Picatinny Arsenal
ATTN: SARPA-TS-S, #59
Dover, NJ 07801

Commanding Officer
Harry Diamond Laboratory
ATTN: Library
2800 Powder Mill Road
Adelphi, MD 20783

Commander
US Army Electronics Command
ATTN: DRSEL-RD-D
Fort Monmouth, NJ 07703

Naval Surface Weapons Center
Code DT 21 (Ms. Greeley)
Dahlgren, VA 22448

Air Force Weapons Laboratory
ATTN: Technical Library (SUL)
Kirtland AFB, NM 87117

Director
US Army Engr Waterways Exper Sta
ATTN: Library Branch
Vicksburg, MS 39180

Commander
US Army Electronics Command
ATTN: DRSEL-CT-D
Fort Monmouth, NJ 07703

Meteorologist in Charge
Kwajalein Missile Range
PO Box 67
APO
San Francisco, CA 96555

Environmental Protection Agency
Meteorology Laboratory
Research Triangle Park, NC 27711

Chief, Technical Services Div
DCS/Aerospace Sciences
ATTN: AWS/DNTI
Scott AFB, IL 62225

Air Force Cambridge Rsch Labs
ATTN: LCH (A. S. Carten, Jr.)
Hanscom AFB
Bedford, MA 01731

Department of the Air Force
16WS/DO
Fort Monroe, VA 23651

Director
US Army Ballistic Research Lab
ATTN: DRXBR-AM
Aberdeen Proving Ground, MD 21005

Geophysics Division
Code 3250
Pacific Missile Test Center
Point Mugu, CA 93042

National Center for Atmos Res
NCAR Library
PO Box 3000
Boulder, CO 80303

William Peterson
Research Association
Utah State University, UNC 48
Logan, UT 84322

Commander
US Army Dugway Proving Ground
ATTN: MT-S
Dugway, UT 84022

Head, Rsch and Development Div (ESA-131)
Meteorological Department
Naval Weapons Engineering Support Act
Washington, DC 20374

Commander
US Army Engineer Topographic Lab
(STINFO CENTER)
Fort Belvoir, VA 22060

Commander
US Army Missile Command
ATTN: DRSMI-RRA, Bldg 7770
Redstone Arsenal, AL 35809

Air Force Avionics Lab
ATTN: AFAL/TSR
Wright-Patterson AFB, Ohio 45433

Commander
US Army Electronics Command
ATTN: DRSEL-VL-D
Fort Monmouth, NJ 07703

Commander
USAICS
ATTN: ATSI-CTD-MS
Fort Huachuca, AZ 85613

E&R Center
Bureau of Reclamation
ATTN: Bldg 67, Code 1210
Denver, CO 80225

HQDA (DAEN-RDM/Dr. De Percin)
Forrestal Bldg
Washington, DC 20314

Commander
Air Force Weapons Laboratory
ATTN: AFWL/WE
Kirtland AFB, NM 87117

Commander
US Army Satellite Comm Agc
ATTN: DRCPM-SC-3
Fort Monmouth, NJ 07703

Commander
US Army Electronics Command
ATTN: DRSEL-MS-TI
Fort Monmouth, NJ 07703

Commander
US Army Electronics Command
ATTN: DRSEL-GG-TD
Fort Monmouth, NJ 07703

Dr. Robert Durrenberger
Dir, The Lab of Climatology
Arizona State University
Tempe, AZ 85281

Commander
Headquarters, Fort Huachuca
ATTN: Tech Ref Div
Fort Huachuca, AZ 85613

Field Artillery Consultants
1112 Becontree Drive
ATTN: COL Buntyn
Lawton, OK 73501

Commander
US Army Nuclear Agency
ATTN: ATCA-NAW
Building 12
Fort Bliss, TX 79916

Director
Atmospheric Physics & Chem Lab
Code 31, NOAA
Department of Commerce
Boulder, CO 80302

Dr. John L. Walsh
Code 5503
Navy Research Lab
Washington, DC 20375

Commander
US Army Electronics Command
ATTN: DRCDE-R
5001 Eisenhower Avenue
Alexandria, VA 22304

Marine Corps Dev & Educ Cmd
Development Center
ATTN: Cmd, Control, & Comm Div (C^3)
Quantico, VA 22134

Commander
US Army Electronics Command
ATTN: DRSEL-WL-D1
Fort Monmouth, NJ 07703

Commander
US Army Missile Command
ATTN: DRSMI-RFGA, B. W. Fowler
Redstone Arsenal, AL 35809

Dir of Dev & Engr
Defense Systems Div
ATTN: SAREA-DE-DDR
H. Tannenbaum
Edgewood Arsenal, APG, MD 21010

Mr. William A. Main
USDA Forest Service
1407 S. Harrison Road
East Lansing, MI 48823

Naval Surface Weapons Center
Technical Library and Information
Services Division
White Oak, Silver Spring, MD 20910

Dr. A. D. Belmont
Research Division
PO Box 1249
Control Data Corp
Minneapolis, MN 55440

Dir, Elec Tech and Devices Lab
US Army Electronics Command
ATTN: DRSEL-TL-D, Bldg 2700
Fort Monmouth, NJ 07703

Director
Development Center MCDEC
ATTN: Firepower Division
Quantico, VA 22134

Commander
US Army Proving Ground
ATTN: Technical Library, Bldg 2100
Yuma, AZ 85364

US Army Liaison Office
MIT-Lincoln Lab, Library A-082
PO Box 73
Lexington, MA 02173

Library-R-51-Tech Reports
Environmental Research Labs
NOAA
Boulder, CO 80302

Head, Atmospheric Research Section
National Science Foundation
1800 G. Street, NW
Washington, DC 20550

Commander
US Army Missile Command
ATTN: DRSMI-RR
Redstone Arsenal, AL 35809

Commandant
US Army Field Artillery School
ATTN: Met Division
Fort Sill, OK 73503

Meteorology Laboratory
AFCRL/LY
Hanscom AFB
Bedford, MA 01731

Commander
US Army Air Defense School
ATTN: C&S Dept, MSLSCI Div
Fort Bliss, TX 79916

Director National Security Agency
ATTN: TDL (C513)
Fort George G. Meade, MD 20755

USAF EPAC/CBT (Stop 825)
ATTN: Mr. Burgmann
Scott AFB, IL 62225

Armament Dev & Test Center
ADTC (DLOSL)
Eglin AFB, Florida 32542

Commander
US Army Ballistic Rsch Labs
ATTN: DRXBR-IB
Aberdeen Proving Ground, MD 21005

Director
Naval Research Laboratory
Code 2627
Washington, DC 20375

Commander
Naval Elect Sys Cmd HQ
Code 51014
Washington, DC 20360

The Library of Congress
ATTN: Exchange & Gift Div
Washington, DC 20540
2

CO, US Army Tropic Test Center
ATTN: STETC-MO-A (Tech Lib)
APO New York 09827

Commander
Naval Electronics Lab Center
ATTN: Library
San Diego, CA 92152

Office, Asst Sec Army (R&D)
ATTN: Dep for Science & Tech
Hq, Department of the Army
Washington, DC 20310

Director
US Army Ballistic Research Lab
ATTN: DRXBR-AM, Dr. F. E. Niles
Aberdeen Proving Ground, MD 21005

Commander
Frankford Arsenal
ATTN: Library, K2400, Bldg 51-2
Philadelphia, PA 19137

Director
US Army Ballistic Research Lab
ATTN: DRXBR-XA-LB
Bldg 305
Aberdeen Proving Ground, MD 21005

Dir, US Naval Research Lab
Code 5530
Washington, DC 20375

Commander
Office of Naval Research
Code 460-M
Arlington, VA 22217

Commander
Naval Weather Service Command
Washington Navy Yard
Bldg 200, Code 304
Washington, DC 20374

Technical Processes Br
D823
Room 806, Libraries Div NOAA
8060 13th St
Silver Spring, MD 20910

The Environmental Rsch Institute of MI
ATTN: IRIA Library
PO Box 618
Ann Arbor, MI 48107

Redstone Scientific Info Center
ATTN: Chief, Documents
US Army Missile Command
Redstone Arsenal, AL 35809

Commander
Edgewood Arsenal
ATTN: SAREA-TS-L
Aberdeen Proving Ground, MD 21010

Sylvania Elec Sys Western Div
ATTN: Technical Reports Library
PO Box 205
Mountain View, CA 94040

Commander
US Army Security Agency
ATTN: IARD-OS
Arlington Hall Station
Arlington, VA 22212
2

President
US Army Field Artillery Board
Fort Sill, OK 73503

Commandant
US Army Field Artillery School
ATTN: ATSF-TA-R
Fort Sill, OK 73503

CO, USA Foreign Sci & Tech Center
ATTN: DRXST-ISI
220 7th Street, NE
Charlottesville, VA 22901

Commander, Naval Ship Sys Cmd
Technical Library, Rm 3 S-08
National Center No. 3
Washington, DC 20360

Commandant
US Army Signal School
ATTN: ATSN-CD-MS
Fort Gordon, GA 30905

Rome Air Development Center
ATTN: Documents Library
TILD (Bette Smith)
Griffiss Air Force Base, NY 13441

HQ, ESD/DRI/S-22
Hanscom AFB
MA 01731

Commander
Frankford Arsenal
ATTN: J. Helfrich PDSP 65-1
Philadelphia, PA 19137

Director
Defense Nuclear Agency
ATTN: Tech Library
Washington, DC 20305

Department of the Air Force
5WW/DOX
Langley AFB, VA 23665

Commander
US Army Missile Command
ATTN: DRSMI-RER (Mr. Haraway)
Redstone Arsenal, AL 35809

CPT Hugh Albers, Exec Sec
Interdept Committee on Atmos Sci
Fed Council for Sci & Tech
National Sci Foundation
Washington, DC 20550

US Army Research Office
ATTN: DRXRO-IP
PO Box 12211
Research Triangle Park, NC 27709

Commander
US Army Training & Doctrine Cmd
ATTN: ATCD-SC
Fort Monroe, VA 23651

Mil Assistant for Environmental Sciences
OAD (E & LS), 3D129
The Pentagon
Washington, DC 20301

Commander
Eustis Directorate
US Army Air Mobility R&D Lab
ATTN: Technical Library
Fort Eustis, VA 23604

National Weather Service
National Meteorological Center
World Weather Bldg - 5200 Auth Rd
ATTN: Mr. Quiroz
Washington, DC 20233

Commander
US Army Materiel Command
ATTN: DRCRD-SS (Mr. Andrew)
Alexandria, VA 22304

Commander
Frankford Arsenal
ATTN: SARFA-FCD-O, Bldg 201-2
Bridge & Tarcony Sts
Philadelphia, PA 19137

Inge Dirmhirn, Professor
Utah State University, UMC 48
Logan, UT 84322

Chief, Aerospace Environ Div
Code ES41
NASA
Marshall Space Flight Center, AL 35802

Dr. Frank D. Eaton
PO Box 3038
University Station
Laramie, Wyoming 82071

Commander
US Army Arctic Test Center
ATTN: STEAC-OP-PL
APO Seattle 98733

Commander
US Army Electronics Command
ATTN: DRSEL-GS-H (Stevenson)
Fort Monmouth, NJ 07703

Commander
USACACDA
ATTN: ATCA-CCC-W
Fort Leavenworth, KS 66027

Commander
US Army Test & Eval Cmd
ATTN: DRSTE-FA
Aberdeen Proving Ground, MD 21005

Air Force Cambridge Rsch Labs
ATTN: LKI
L. G. Hanscom Field
Bedford, MA 01730

Director, Systems R&D Service
Federal Aviation Administration
ATTN: ARD-54
2100 Second Street, SW
Washington, DC 20590

USAFETAC/CB (Stop 825)
Scott AFB
IL 62225

Director
USAE Waterways Experiment Station
ATTN: Library
PO Box 631
Vicksburg, MS 39180

Defense Documentation Center
ATTN: DDC-TCA
Cameron Station (BLDG 5)
Alexandria, Virginia 22314
12

Commander
US Army Electronics Command
ATTN: DRSEL-CT-S
Fort Monmouth, NJ 07703

Commander
Holloman Air Force Base
6585 TG/WE
Holloman AFB, NM 88330

Commandant
USAFAS
ATTN: ATSF-CD-MT (Mr. Farmer)
Fort Sill, OK 73503
2

Commandant
USAFAS
ATTN: ATSF-CD-C (Mr. Shelton)
Fort Sill, OK 73503
2

Commander
US Army Electronics Command
ATTN: DRSEL-CT-S (Dr. Swingle)
Fort Monmouth, NJ 07703

☆ U S GOVERNMENT PRINTING OFFICE: 1977—777-022/11

SUPPLEMENTARY

INFORMATION

ERRATA SHEET FOR ECOM REPORT 5812

APPLICATION OF THE AN/GVS-5 LASER RANGEFINDER TO CLOUD BASE HEIGHT MEASUREMENTS

Make the following changes:

Page 33, APPENDIX B

Line 2 - Substitute $y = a_0 + a_1x$ in lieu of $v = a_0 + a,x$

Line 5 - Substitute a_1 in lieu of a,

Line 6 - Substitute a_1 in lieu of a,

Line 7 - change

$$a_i = \frac{x_i y_i - \frac{\Sigma\, x_i\ \Sigma\, y_i}{n}}{\Sigma\, x_i^2 \quad \frac{(\Sigma x_i)^2}{n}}$$

to read

$$a_1 = \frac{\Sigma\, x_i y_i - \frac{\Sigma\, x_i\ \Sigma\, y_i}{n}}{\Sigma\, x_i^2 - \frac{(\Sigma\, x_i)^2}{n}}$$